AWARD NUMBER: W81XWH-16-2-0029

TITLE: Role of Matrix Metalloproteinase-3 in Deployment-Related Pulmonary Fibrosis

PRINCIPAL INVESTIGATOR: Gregory P. Downey

CONTRACTING ORGANIZATION: NATIONAL JEWISH HEALTH
DENVER, CO

REPORT DATE: December 2020

TYPE OF REPORT: Final Report

PREPARED FOR: U.S. Army Medical Research and Development Command
Fort Detrick, Maryland 21702-5012

REPORT DOCUMENTATION PAGE

Form Approved
OMB No. 0704-0188

1. REPORT DATE	**2. REPORT TYPE**	**3. DATES COVERED**
December 2020	Final Report	15Aug2016-14Aug2020

4. TITLE AND SUBTITLE

Role of Matrix Metalloproteinase-3 in Deployment-Related Pulmonary Fibrosis

5a. CONTRACT NUMBER
W81XWH-16-2-0029

5b. GRANT NUMBER

5c. PROGRAM ELEMENT NUMBER

6. AUTHOR(S)

Downey, Gregory P., MD & Radisky, Derek C., PhD

E-Mail: DowneyG@NJHealth.org

5d. PROJECT NUMBER

5e. TASK NUMBER

5f. WORK UNIT NUMBER

7. PERFORMING ORGANIZATION NAME(S) AND ADDRESS(ES)

NATIONAL JEWISH HEALTH
1400 JACKSON ST
DENVER CO 80206-2761

8. PERFORMING ORGANIZATION REPORT

9. SPONSORING / MONITORING AGENCY NAME(S) AND ADDRESS(ES)

U.S. Army Medical Research and Development Command, 820 Chandler Street, Fort Detrick, Maryland 21702-5012

10. SPONSOR/MONITOR'S ACRONYM(S)

11. SPONSOR/MONITOR'S REPORT NUMBER(S)

12. DISTRIBUTION / AVAILABILITY STATEMENT

Approved for Public Release; Distribution Unlimited

13. SUPPLEMENTARY NOTES
N/A

14. ABSTRACT
We have demonstrated that exposure of mice to silicate-containing PM induces pulmonary fibrosis with initial inflammation in the terminal bronchioles and alveolar ducts followed by collagen deposition. We have demonstrated that human alveolar macrophages respond to inhaled particulate matter by producing an array of inflammatory and fibrogenic mediators that likely contribute to the respiratory symptoms and clinical illness frequently observed in military personnel previously deployed to Southwest Asia and Afghanistan.

We have demonstrated the feasibility of engineering highly selective TIMP-based MMP inhibitors by yeast surface display. We expect this result to impact the field of protein engineering. Our efforts to uncover the sequence and structural determinants responsible for improvements in TIMP-1 selectivity will also impact the understanding of protein-protein interactions and binding specificity.

15. SUBJECT TERMS
Pulmonary fibrosis; lung injury; matrix metalloproteinases; tissue inhibitors of metalloproteinases; airborne particulate matter; bronchiolitis; field emission scanning electron microscopy; inductively coupled plasma mass spectrometry; immunohistochemistry.

16. SECURITY CLASSIFICATION OF:			**17. LIMITATION OF ABSTRACT**	**18. NUMBER OF PAGES**	**19a. NAME OF RESPONSIBLE PERSON**
					USAMRMC
a. REPORT	**b. ABSTRACT**	**c. THIS PAGE**			**19b. TELEPHONE NUMBER** *(include area code)*
Unclassified	Unclassified	Unclassified	Unclassified	35	

Standard Form 298 (Rev. 8-98)
Prescribed by ANSI Std. Z39.18

TABLE OF CONTENTS

1. INTRODUCTION:

Since the onset of military operations in Afghanistan in 2001 and Iraq in 2003 through Operations Iraqi Freedom, Enduring Freedom, and New Dawn (OIF/OEF/OND), more than 2.8 million military personnel, DoD contractors, US government, and NGO employees have been deployed to these regions. These personnel have been exposed to high levels of airborne particulate matter (PM; 'desert dust') generated by wind erosion of desert sand, movement of vehicles and troops, combustion and construction activities, and combat, with both short and long-term health consequences. In deployed military personnel, high levels of PM have been causally implicated in the observed increase in respiratory symptoms, asthma, bronchiolitis, and eosinophilic and interstitial lung disease. The goal of this application is to determine the mechanisms by which inhalational exposure to silicate-containing respirable PM during military deployment to Southwest Asia leads to chronic pulmonary inflammation and fibrosis and to investigate strategies to diagnose and repair this damage. Aim 1 is to determine the role of MMP-3 in preclinical (murine) models of pulmonary fibrosis induced by instillation of bleomycin, silica, or silicate-containing particulate matter (PM) from Iraq and Afghanistan. Aim 2 is to develop an MMP-3-selective Tissue Inhibitor of Metalloproteinase (TIMP) as therapeutic target for progressive pulmonary fibrosis using both *in silico* and *in vitro* approaches. Aim 3 is to determine if MMP-3 levels are elevated in the lungs and blood of patients with pulmonary fibrosis and in military personnel previously deployed to Southwest Asia and can be used as a biomarker for disease progression.

2. KEYWORDS:

Pulmonary fibrosis; lung injury; matrix metalloproteinases; tissue inhibitors of metalloproteinases; airborne particulate matter; bronchiolitis; field emission scanning electron microscopy; inductively coupled plasma mass spectrometry; immunohistochemistry.

3. ACCOMPLISHMENTS:

What were the major goals of the project?

Major Task 1: Define the role of MMP-3 in PM-induced pulmonary fibrosis.
Milestone: ACURO Approval 6 Months Achieved
Milestone: **Major Task 1** **Milestone:** Achieved by 36 months

Major Task 2: Develop an MMP-3-selective tissue inhibitor of metalloproteinase (TIMP) and evaluate its efficacy in animal models of PM-induced pulmonary fibrosis.
Milestone: **Major Task 2** **Milestone:** Achieved by 36 months

Major Task 3: Determine if levels of MMP-3 and MMP-3 proteolytic products are elevated in the lungs and blood of patients with pulmonary fibrosis and in military personnel previously deployed to Southwest Asia and can be used as a biomarker for disease progression.
Milestone: **Major Task 3** **Milestone:** Achieved by 36 months

What was accomplished under these goals?

Major Task 1: Define the role of MMP-3 in PM-induced pulmonary fibrosis

Subtask 1. Obtain Local (National Jewish Health) IACUC Approval

We obtained local (National Jewish Health) IACUC approval on 06/14/2016 (NJH protocol # AS2830-05-19).

Subtask 2. Obtain USAMRMC Animal Care and Use Review Office approval for mouse experiments

We obtained USAMRMC Animal Care and Use Review Office (ACURO) approval for experiments to be conducted at National Jewish Health on 08/3/2016. The protocol was renewed on Sept 10, 2019 for an additional 3 years that allowed us to complete additional experiments during the no cost extension that ended in September 2020.

We collaborated with Drs. Karen Mummy and Brian Wong at NAMRU-Dayton and the protocol was approved by the Wright Patterson Air Force Base IACUC and remained active throughout the study.

Subtask 3. Develop animal models of pulmonary fibrosis induced by intratracheal administration of silicate-containing PM and compare to the standard bleomycin model.

This section will summarize the studies conducted over the course of the grant. We developed several preclinical models of pulmonary fibrosis including (i) single and multiple dose intratracheal (i.t.) bleomycin; (ii) single dose purified silica; and (iii) single and multiple dose i.t. silicate-containing PM from Iraq and Afghanistan. We used these models to determine the importance of MMP-3 in the pathogenesis of pulmonary fibrosis by comparing fibrogenic responses between wild type (WT) and *Mmp3*$^{-/-}$mice.

Initially, we titrated the dose of bleomycin to achieve consistent pulmonary fibrosis as measured biochemically using the hydroxyproline assay or measuring collagen 1 mRNA without excess mortality (**Fig. 1**). In the single dose bleomycin model, *Mmp3*$^{-/-}$mice were largely protected from bleomycin-induced fibrosis compared to WT littermate controls (**Fig. 2**).

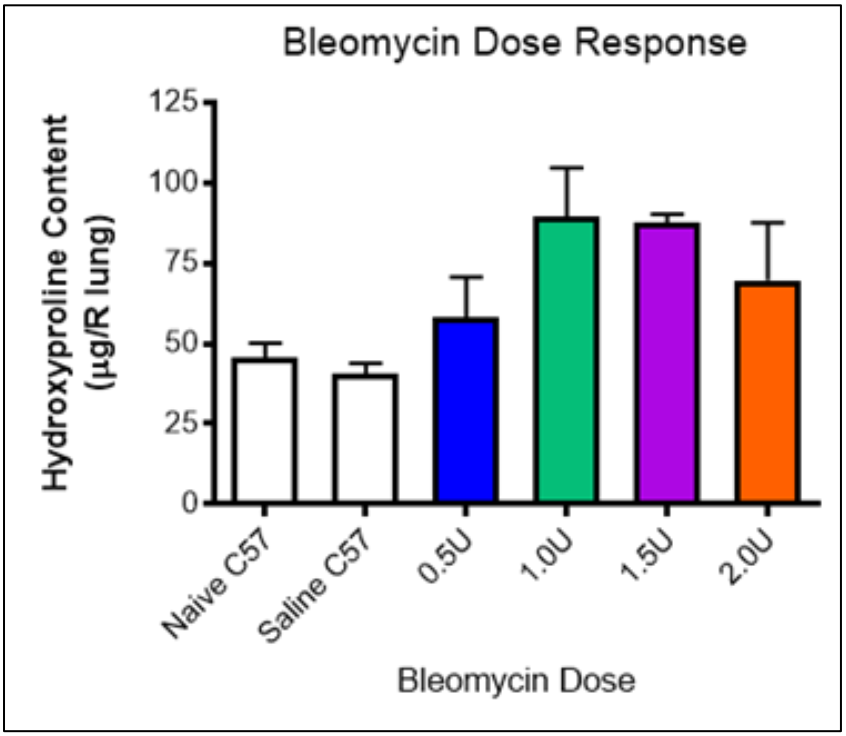

Fig. 1. Single dose intratracheal bleomycin induces dose-dependent lung fibrosis in WT BL/6 mice (n=6-8 per group).

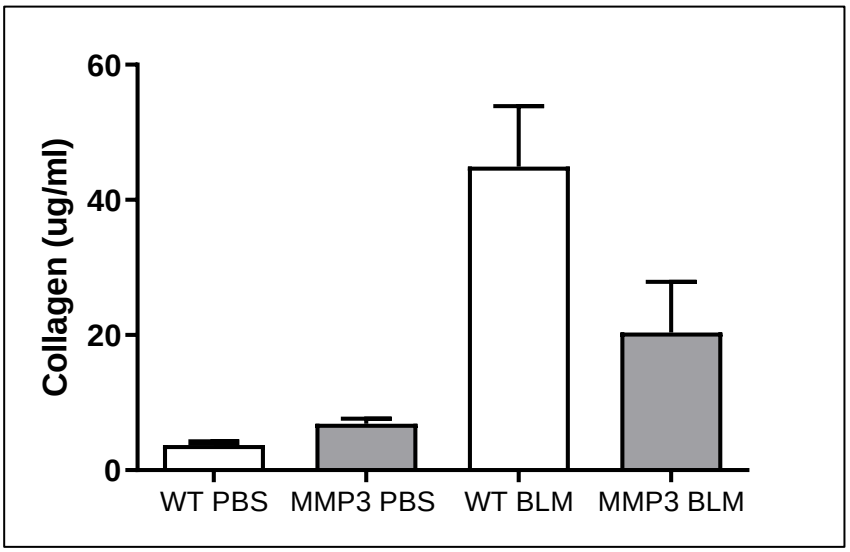

Fig. 2. *Mmp3*$^{-/-}$ mice are protected from bleomycin-induced pulmonary fibrosis compared to WT C57Bl/6 controls (single dose model). Lung collagen is measured using hydroxyproline (n=6 per group).

Similarly, in the multiple-dose bleomycin model, *Mmp3*$^{-/-}$mice were largely protected from bleomycin-induced fibrosis compared to WT littermate controls. Of note is that the multiple dose bleomycin model is considered to be more reflective of human pulmonary fibrosis than is the single dose model.

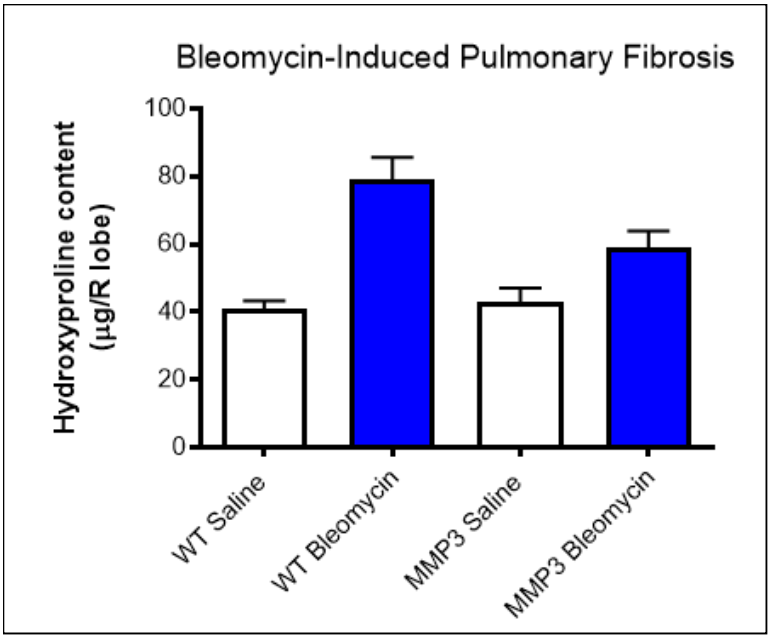

Fig. 3. *Mmp3* null mice (MMP3) are protected from lung fibrosis in the multiple-dose bleomycin model compared to WT C57Bl/6 controls (n=6-8 per group).

We next sought to determine whether *Mmp3*$^{-/-}$mice were protected from pulmonary fibrosis induced by instillation of particulate matter (PM). We began using purified silica that is known to induce pulmonary fibrosis. We tested 5 µm diameter silica from three different sources: NIST, NanoAmor (amorphous silica) and US Silica (Minusil: structured crystalline silica). **Fig 4** illustrates the size distribution of the purified silica confirming the stated mean diameter of 5 µm.

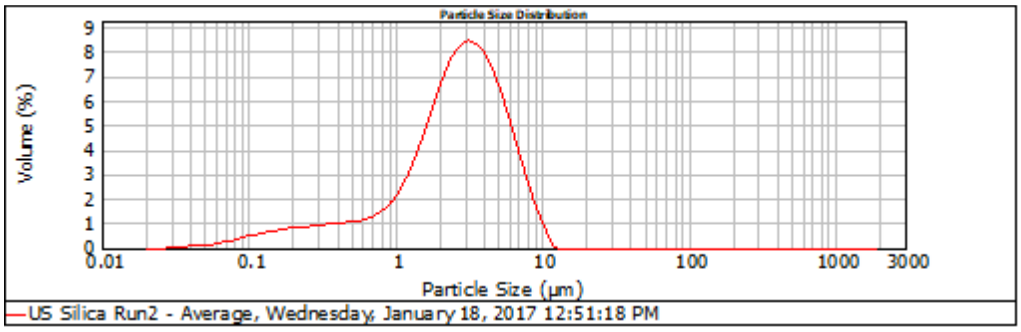

Fig. 4. Size distribution of purified silica

Initially we delivered the purified silica (200 mg/kg) directly into the lung using either intratracheal instillation or oropharyngeal aspiration (OPA) to ensure optimal intrapulmonary delivery of the silica. We found that OPA gave the most consistent results in terms of induction of pulmonary fibrosis as determined by lung hydroxyproline content (**Fig. 5**). Histologically, the silica induced a granulomatous reaction in the lung **(Fig. 6)** and localized fibrosis (**Fig. 7**) as anticipated.

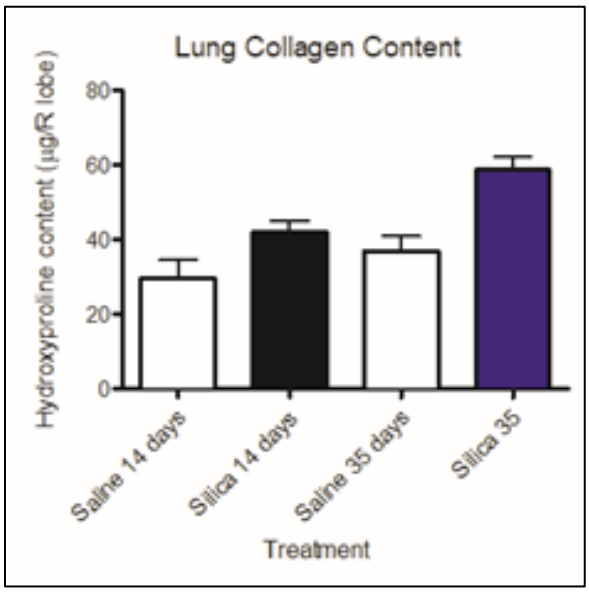

Fig. 5. Increase in lung collagen content in WT C57BL/6 mice induced by direct intrapulmonary silica instillation as measured by hydroxyproline content (n=6 per group).

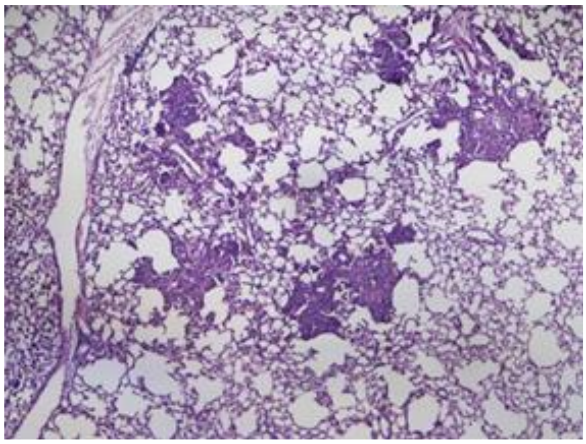

Fig. 6. Formation of granuloma in lungs of mice given silica by i.t. instillation (H&E stain: 4 X magnification).

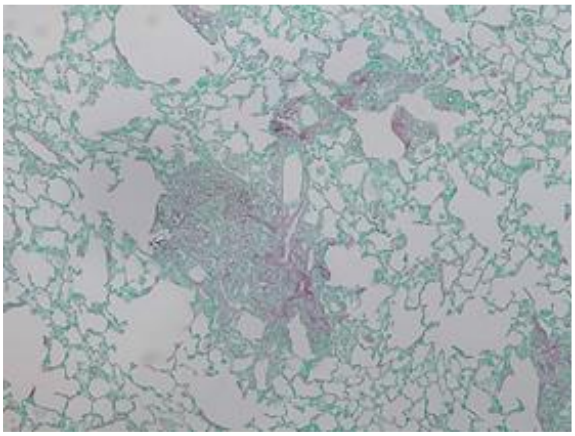

Fig. 7. Formation of granuloma containing increased collagen in lungs of mice given silica by i.t. instillation (picrosirius red stain; 10 X magnification).

In contrast to the bleomycin model, *Mmp3*$^{-/-}$ mice were not protected from pulmonary fibrosis induced by intrapulmonary instillation silica (**Fig. 8**). We also observed that the degree of pulmonary fibrosis induced in WT mice was similar whether we used crystalline (Minusil) or amorphous (NanoAmor) silica (not illustrated).

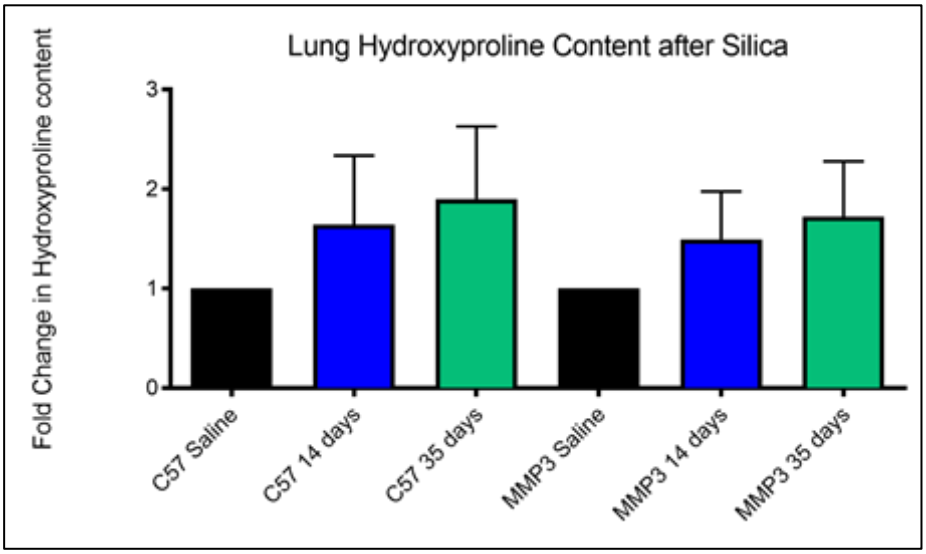

Fig. 8. Comparison of the degree of lung fibrosis at days 14 and 35 between WT (C57BL/6) and *Mmp3* null mice (MMP3) in response to intratracheal instillation of silica (n=6 per group).

We next sought to determine whether intrapulmonary administration of silicate-containing particulate matter (PM) from Iraq and Afghanistan induced pulmonary fibrosis. PM from the inland desert area of California (China Lake) was used as a 'control' to determine whether the pulmonary effects were related to the geographical source of the PM. The PM from Iraq were collected from high volume air sampling filters in theater near Baghdad airport (Camp Victory). The PM from Afghanistan was generated from topsoil collected from Bagram Air Force Base by the US Army Core of Engineers and then transported back to the United States, sterilized by autoclaving, and then aerosolized and collected on Teflon filters in the inhalation toxicology facility at NAMRU-Dayton on the Wright Peterson Air Force base. The mean diameter of these sources of PM was 5 µm, comparable to mean diameter of the PM from Iraq.

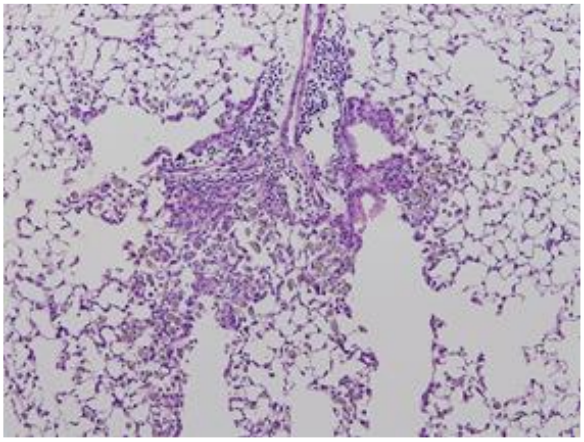

Fig. 9. Instillation of multiple doses of PM from Iraq or Afghanistan induces inflammation centered on the terminal bronchioles and alveolar ducts. PM can be identified in macrophages in these areas (H&E: 20 X magnification)

Initial experiments used a single dose 5 mg/kg of PM delivered by oropharyngeal aspiration with end points at 14 and 35 days. These studies demonstrated a variable increase in lung collagen content from PM from Iraq and Afghanistan that did not achieve statistical significance. We next studied the effects of multiple sequential instillations of PM (5 doses of 5 mg/kg given every other day for 10 days) with end points at 14 and 35 days after the last instillation. **Fig. 9** illustrates that intrapulmonary instillation of multiple doses of PM from Iraq and Afghanistan induced inflammation centered on the terminal bronchioles and alveolar ducts. **Fig. 10** illustrates that multiple sequential instillations of PM from Iraq and Afghanistan induced significant pulmonary fibrosis in a dose-dependent manner. PM from Afghanistan induced the highest degree of pulmonary fibrosis whereas PM from California did not induce significant pulmonary fibrosis in these experiments **(Fig. 10)**.

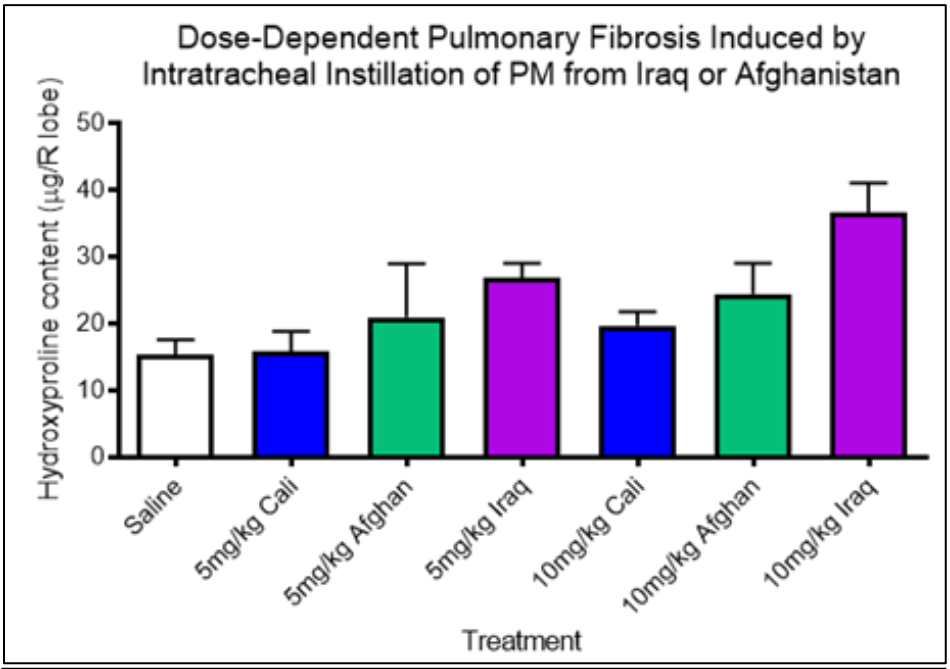

Fig. 10. Five doses of PM from Iraq or Afghanistan but not California (Cali) given every other day for 10 days induces dose-dependent lung fibrosis in WT type C57BL/6 mice (n=6-8 per group).

We next sought to determine whether *Mmp3*$^{-/-}$mice were protected from pulmonary fibrosis induced by instillation of particulate matter (PM). For these experiments, we compared the fibrogenic effects of PM from Afghanistan and California (China Lake) administered into the lung by oropharyngeal aspiration (OPA). PM from Iraq was not included in these experiments because supplies were very limited at the time these experiments were conducted. **Fig 11** illustrates that *Mmp3*$^{-/-}$mice were not protected from pulmonary fibrosis induced by instillation of silicate containing PM from Afghanistan. In fact, *Mmp3*$^{-/-}$ mice exhibited higher degrees of fibrosis in response to intrapulmonary administration of Afghanistan PM compared to WT mice and *Mmp3*$^{-/-}$mice developed pulmonary fibrosis in response to intrapulmonary administration of PM from China Lake.

To determine if there were sex-specific fibrogenic responses to PM exposure, we compared responses in male and female mice (**Figs. 12 and 13**). However, both male and female mice responded similarly to PM exposure.

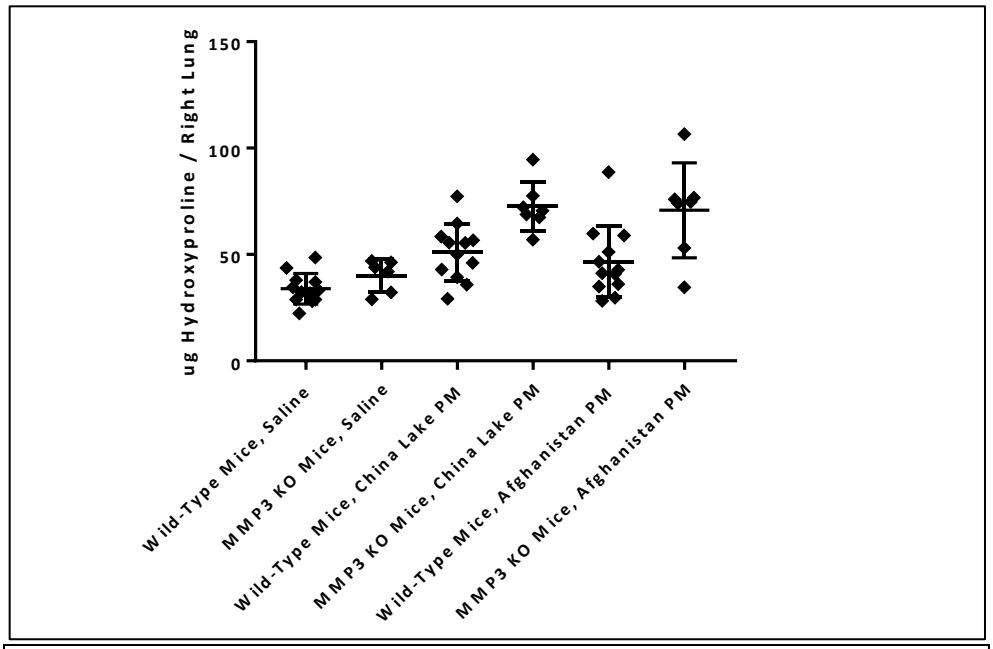

Fig. 11. Comparison of the degree of lung fibrosis at day 35 between WT (C57BL/6) and *Mmp3*$^{-/-}$ mice (MMP3 KO) in response to intrapulmonary delivery of PM from Afghanistan and California (China Lake) (n=12).

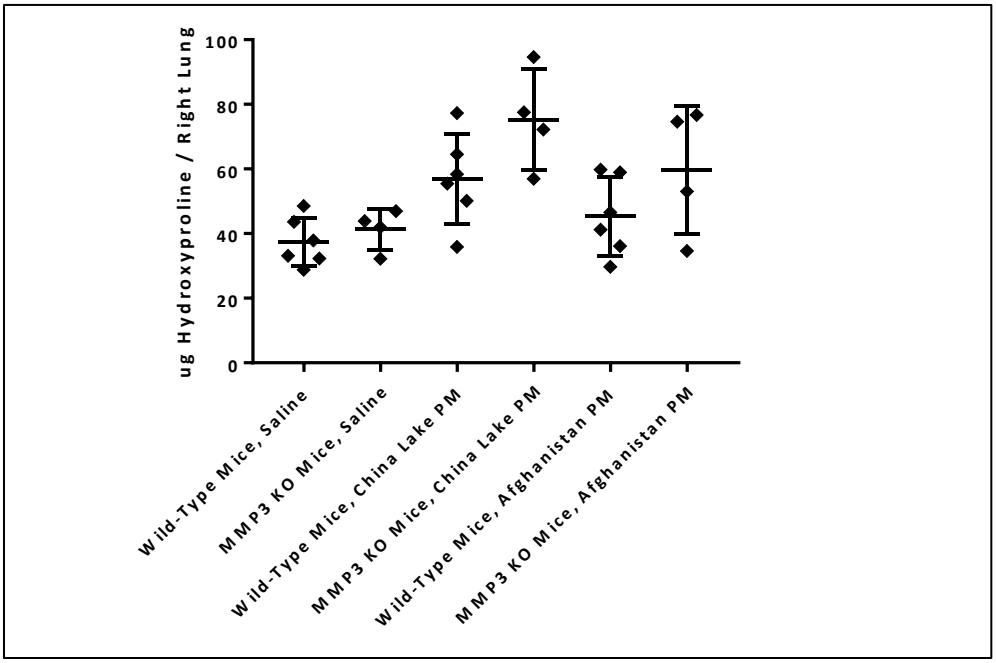

Fig. 12. Comparison of lung fibrosis at day 35 between male WT (C57BL/6) and *Mmp3*$^{-/-}$ mice (MMP3 KO) in response to intrapulmonary delivery of PM from Afghanistan and California (China Lake) (n=6).

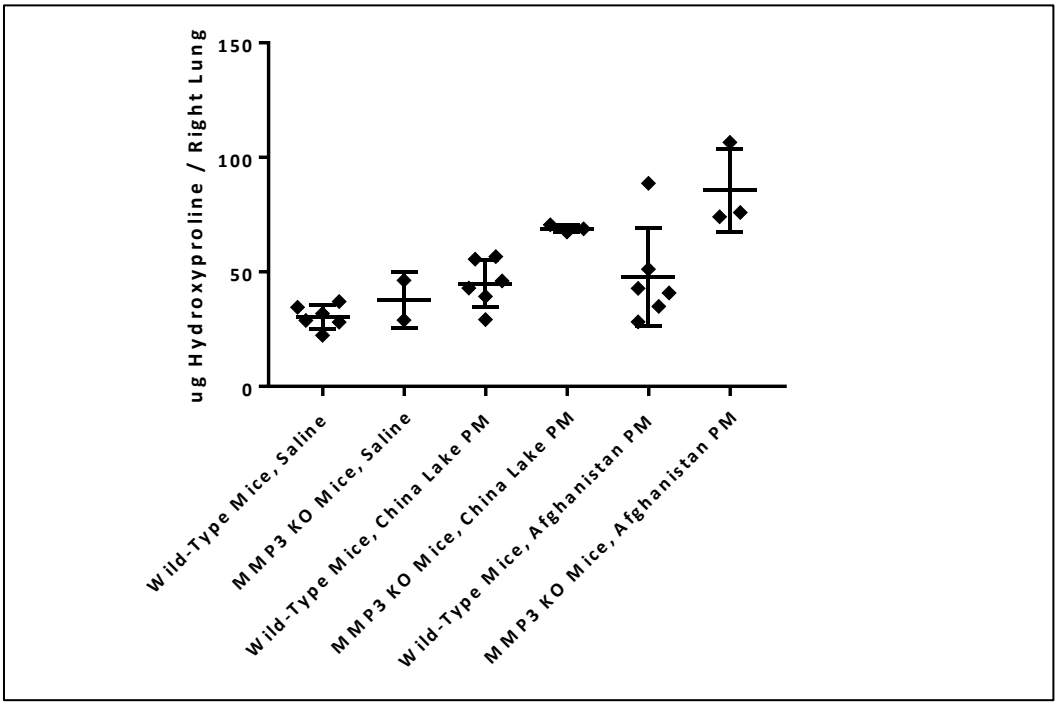

Fig. 13. Comparison of lung fibrosis at day 35 between female WT (C57BL/6) and *Mmp3*$^{-/-}$ mice (MMP3 KO) in response to intrapulmonary delivery of PM from Afghanistan and California (China Lake) (n=6).

To summarize the results of this section, we observed that *Mmp3*$^{-/-}$mice are protected from pulmonary fibrosis induced by single dose or multiple dose intrapulmonary bleomycin whereas they are not protected from pulmonary fibrosis induced by either purified silica or by silicate-containing PM from Afghanistan. These observations provide evidence that different mechanisms drive fibrosis in response to bleomycin (bleomycin-induced fibrosis is likely dependent on initial epithelial injury followed by production of fibrogenic mediators from the injured epithelial cells) compared to fibrosis driven by purified silica or silicate-containing PM. The latter is likely driven by fibrogenic mediators produced by macrophages that ingest the particulate matter and then produce fibrogenic mediators.

Subtask 4. Develop animal models of pulmonary fibrosis induced by aerosolized silicate-containing PM.

Over the course of this study, we undertook three large experiments designed to characterize the effects of aerosol exposure to purified silica and to PM from Afghanistan and purified silica at the NAMRU-Dayton/Wright Patterson Air Force Base inhalation toxicology facility in collaboration with our co-investigators Drs. Karen Mumy and Brian Wong. The first set of exposure experiments (n= 344 mice) were conducted in whole body aerosolization chambers using a protocol that had been developed for exposure of rats to aerosolized PM (5 mg/m3 for 20 hr/day, 5 d/week, over 4 weeks, for a total of 20 exposure days). Mice were then shipped to National Jewish Health in Denver for end point analysis 3 days later. As illustrated below in **Figs. 14 and 15**, aerosol exposure to PM from Afghanistan or California or to silica resulted in lung inflammation as measured by an increase in BAL cell counts (**Fig. 14**) but a relatively

minimal increase in lung collagen content (**Fig. 15**). No differences between the wild-type and *Mmp3-/-* mice were observed.

Given the absence in significant lung fibrosis from the initial protocol, we redesigned the exposure protocol based on published studies from other groups (using rats) who used a higher dose and allowed a longer period of time (up to 90 days) after the completion of exposures that would allow fibrosis to develop. A second aerosol exposure experiment using a higher concentration of PM (70 mg/m^3, 5 h/day, for 12 days) was conducted at NAMRU-Dayton and the mice were shipped to National Jewish Health for end point analysis. The mice were euthanized at 2, 4, and 8 weeks after exposure. We observed evidence of lung inflammation (increase in total cell counts in BAL fluid) but no evidence of lung fibrosis (**Fig. 16**). We interpreted this to mean that the efficiency of the mouse nasopharynx at removing aerosolized PM prevents much of the PM from accessing the lung and thus there was no measurable fibrotic response.

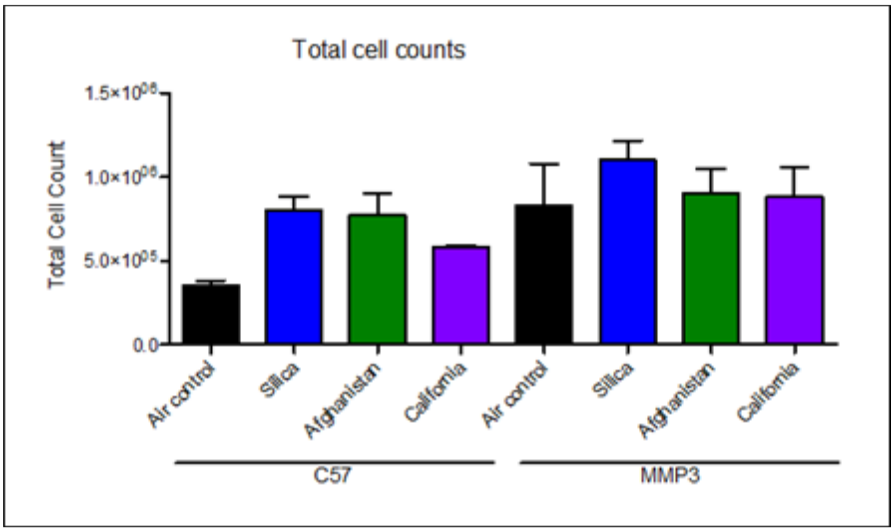

Fig. 14. Aerosol exposure to PM from Afghanistan or California (China Lake) or to purified crystalline silica resulted in lung inflammation by as measured increased total cells in BAL fluid.

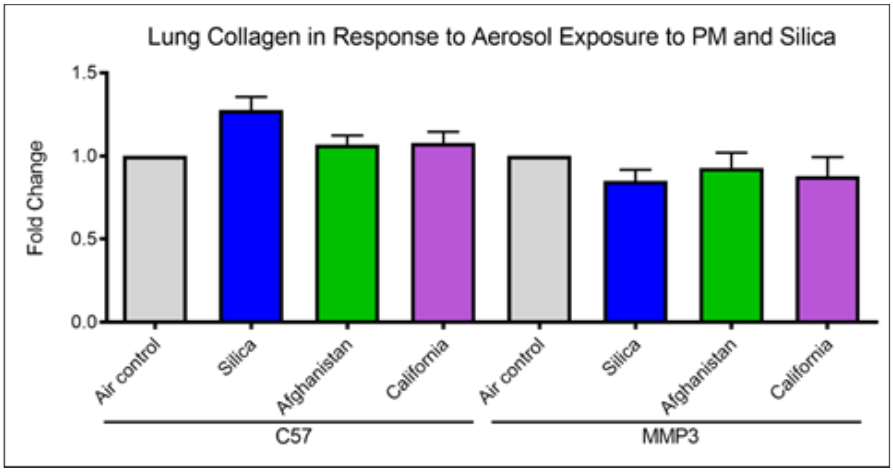

Fig. 15. Minimal increase in lung collagen content induced by aerosol exposure to silica as measured by hydroxyproline.

We again modified the protocol to include a 12-week time point based on the rationale that fibrosis may take longer to develop than 8 weeks in response to the aerosol exposure protocol. We conducted a third large experiment with aerosol exposure to PM (70 mg/m^3, 5 h/day, for 12 days) at NAMRU-Dayton and the mice were shipped to National Jewish Health for end point

analysis. We euthanized the mice at 4, 8, and 12 weeks and conducted BAL to measure inflammation and assessed lung fibrosis using hydroxyproline. Again we observed evidence of lung inflammation (increase in total cell counts in BAL fluid) but no evidence of lung fibrosis even out to 12 weeks (not illustrated). Based on discussions with our program officer, we decided to use the oropharyngeal aspiration method for delivery to the lung for all future experiments.

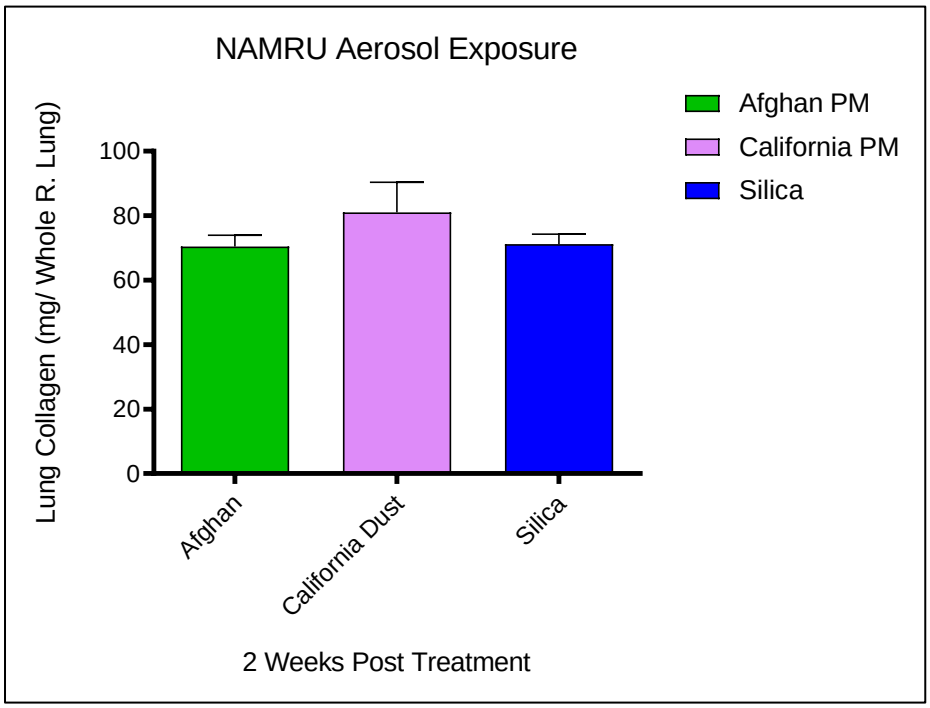

Fig. 16. No increase in lung collagen content induced by aerosol exposure to PM from Afghanistan or California or to purified silica as measured by lung hydroxyproline content.

Subtask 5. Assess osteopontin cleavage in PM-induced fibrosis.

We conducted experiments measuring cleaved fragments of osteopontin in the lungs of mice treated with bleomycin and PM from Southwest Asia. We were able to detect both intact osteopontin and several smaller Mr proteolytic fragments (not illustrated). There were no apparent differences in the abundance of the proteolytic fragments between WT and *Mmp3*$^{-/-}$ mice. Thus there appear to be other proteinases (i.e. besides MMP3) that are able to cleave osteopontin.

We have conducted a series of experiments looking at the potentially inflammatory and fibrogenic mediators released in mouse lung in response to silica exposure. We have been able to detect increased levels of interleukin-(IL)1β, tumor necrosis factor (TNF)α, and osteopontin mRNA after silica exposure (**Figs. 17, 18, and 19**). Responses were comparable or even amplified in *Mmp3*$^{-/-}$ compared to WT mice.

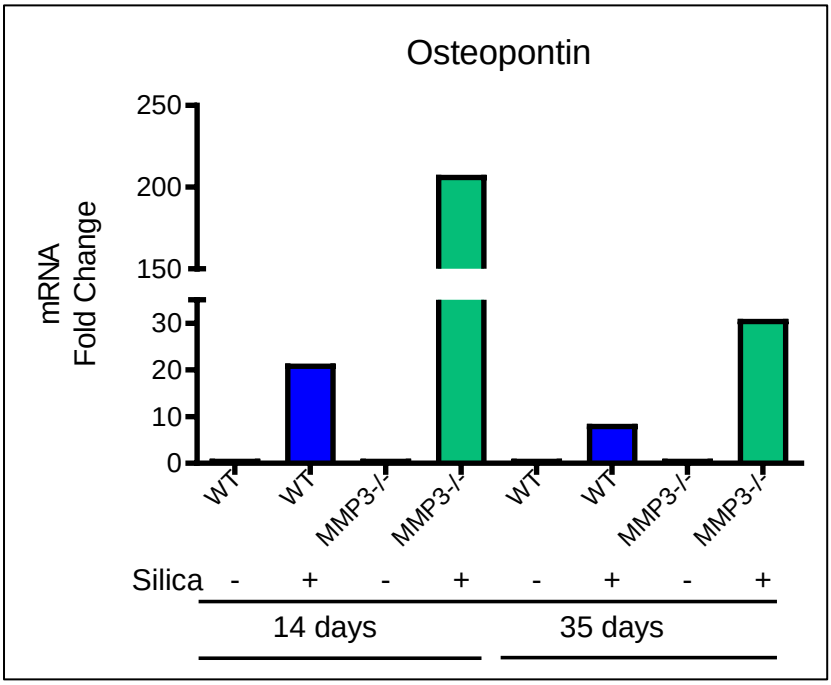

Fig. 17. Levels of osteopontin mRNA in whole lung extracts in WT and *Mmp3*$^{-/-}$ mice in response to silica exposure as determined by qPCR (TaqMan).

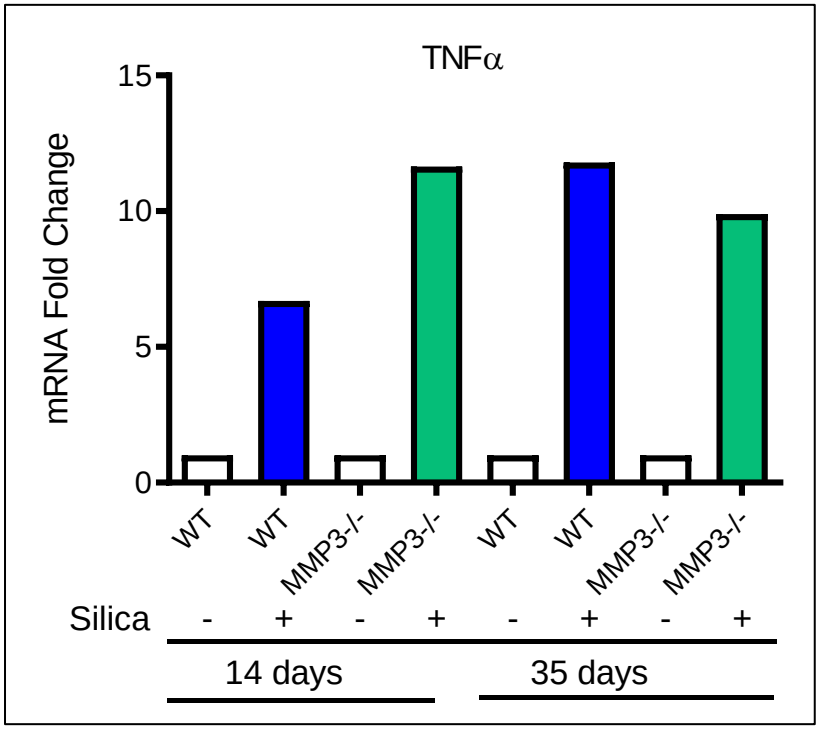

Fig. 18. Levels of TNFα mRNA in whole lung extracts in WT and *Mmp3*$^{-/-}$ mice in response to silica exposure as determined by qPCR (TaqMan).

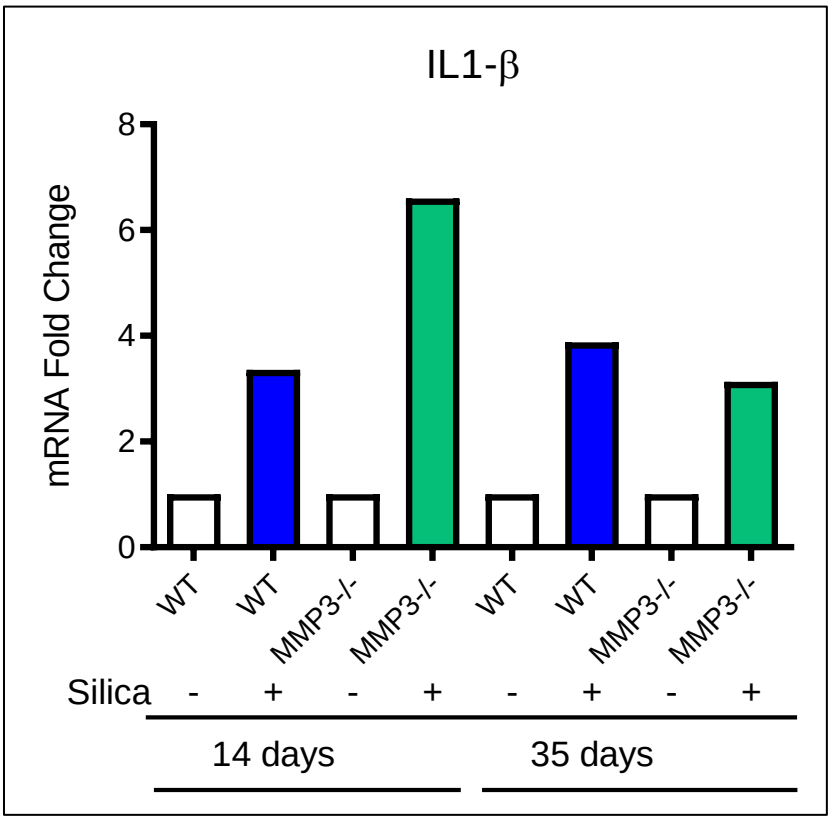

Fig. 19. Levels of IL-1β mRNA in whole lung extracts in WT and *Mmp3*$^{-/-}$ mice in response to silica exposure as determined by qPCR (TaqMan).

Subtask 6. Identify signaling pathways distinctly activated during PM-induced fibrosis by PCR arrays and RNAseq.

We first examined changes in global mRNA expression in whole lung extracts using in WT C57BL/6 mice in response to direct intrapulmonary instillation of multiple dose PM from Iraq and Afghanistan 35 days after the final instillation of PM. Saline was used as a control. **Fig. 20** illustrates that instillation of PM from Iraq and Afghanistan resulted in enhanced expression of a variety of inflammatory and fibrogenic genes including Ccl3 (MIP1α), MMP-13, TNFα, IL1α, IL-10, Lox, Mmp2, Tbfb1, Col3a1, CTGF, Mmp3, Il1β, Il13, Itgb6, and Mmp14.

At this juncture, given that there were no apparent differences in the degree of pulmonary fibrosis between WT and *Mmp3*$^{-/-}$ mice induced by instillation of silicate-containing PM from Southwest Asia or purified silica, we decided not to proceed with whole lung RNAseq analysis of WT and *Mmp3*$^{-/-}$ mice exposed to PM as we felt that this would not be informative

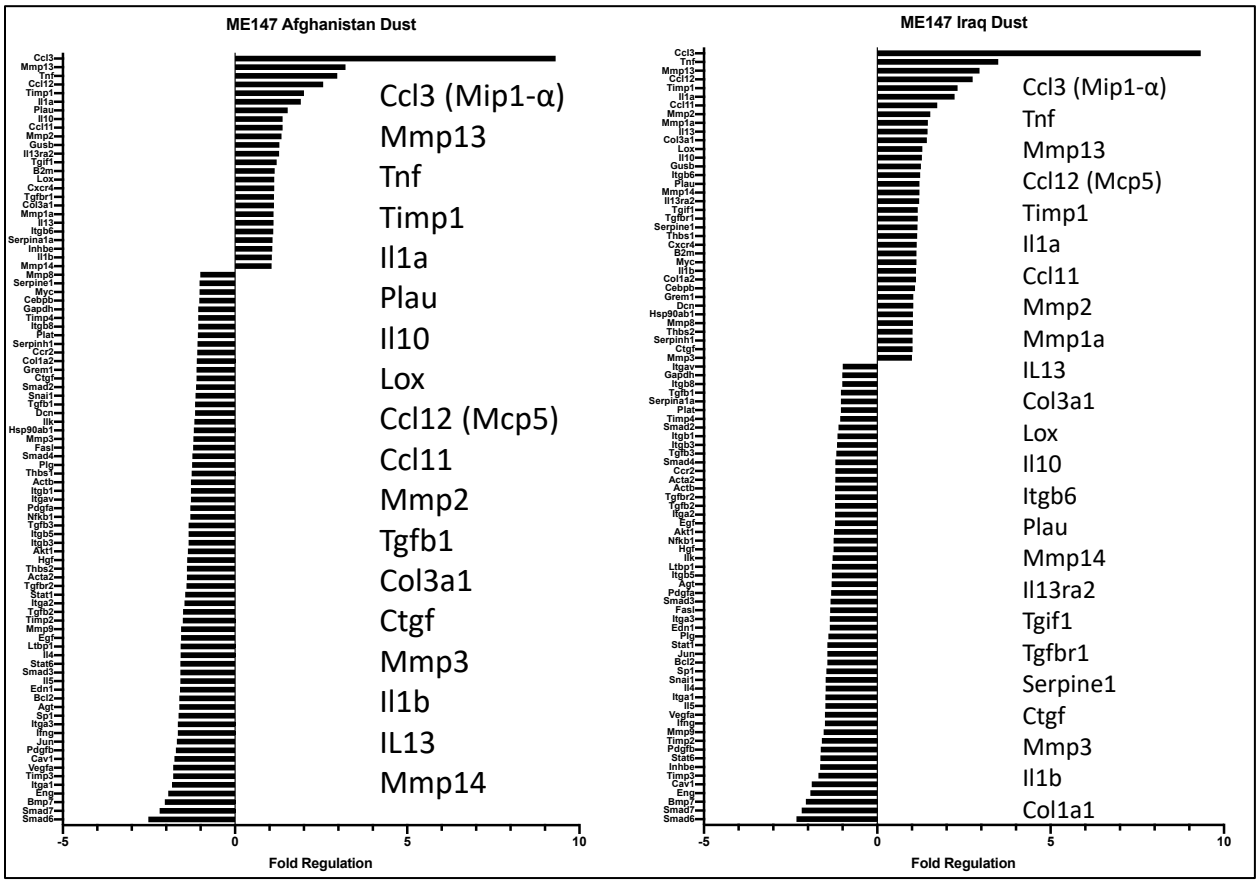

Fig. 20. Transcriptional alterations in whole mouse lung extracts in response to instillation of multiple dose PM (35-day time point) from Iraq and Afghanistan as determined by PCR arrays (QIAGEN).

Subtask 7. Assess fibrogenic response and matrix remodeling in PM-exposed lung fibroblasts.

We developed a reproducible and robust method of isolating fibroblasts from mouse and human lung using a combination of collagenase and Dispase to digest lung followed by negative selection using magnetic beads coated with anti-CD45 and anti-PECAM antibodies to remove hematopoietic cells and epithelial cells. We compared fibrogenic gene expression (Col1a1, EDA-fibronectin, Acta2, and Ccn2) in fibroblasts isolated from WT and *Mmp3*$^{-/-}$ mice at 14 and 35 days after PM and silica exposure. There were no apparent differences between lung fibroblasts isolated from WT and *Mmp3*$^{-/-}$ mice.

Subtask 8. Prepare and submit manuscripts for publication.

We submitted one abstract and published one manuscript related to these studies.

Abstract: Downey GP, Roybal H, Redente E, Aschner Y, Wong M. MMP3 Is Required for Bleomycin- but not Silica-Induced Pulmonary Fibrosis in Experimental Models. Submitted to the 2018 Annual International Conference of the American Thoracic Society.

Manuscript: Raeeszadeh-Sarmazdeh M, Greene KA, Sankaran B, Downey GP, Radisky D, Radisky Y. Directed evolution of metalloproteinase inhibitor TIMP-1 reveals cooperation between domains in matrix metalloproteinase recognition. *J Biol Chem* 2019;294(24):9476-9488. doi: 10.1074/jbc.RA119.008321).

Major Task 2: Develop an MMP-3-selective tissue inhibitor of metalloproteinase (TIMP) and evaluate its efficacy in animal models of PM-induced pulmonary fibrosis (Data in this task are from Dr. Radisky at the Mayo Clinic)

First generation MMP-3 inhibitors based on human TIMP-1. To improve the potency and selectivity of the natural MMP inhibitor TIMP-1 toward MMP-3, we used yeast surface display (YSD) to screen a diversity library of full-length human TIMP-1, as reported in detail in our publication (**Raeeszadeh-Sarmazdeh 2019**). The coding sequence of human TIMP-1 was C-terminally fused to the N-terminus of yeast surface protein Aga2p in the yeast expression vector pCHA. We demonstrated efficient expression and display of the fusion construct, and robust binding to the MMP-3 catalytic domain (MMP-3cd) (**Fig. 21A,B**). We next constructed a YSD diversity library of 5×10^6 independent variants, in which 17 residues located in five discontinuous loops of TIMP-1 (**Fig. 21C**) were partially degenerated, such that each clone contained an average of 4 mutations. We screened this library using fluorescence-activated cell sorting (FACS), identifying "ultra-binders" of MMP-3 possessing affinities enhanced by ~5-10-fold (**Fig. 22A**). Affinity improvements quantified in the YSD context were validated by MMP-3 inhibition studies using purified soluble recombinant TIMP variants, with consistent results showing improved inhibition constants in the low picomolar range. Sequencing of ultra-binder variants revealed that most contained 3-5 mutations, distributed among the diversified loops (**Fig. 22B**). Interestingly, we noted that frequent mutation L34G, located in the N-terminal domain, often co-occurred with mutations of residue Gly154, located >30 Å away in the C-terminal domain. We probed the functional interaction of these distant residues through mutagenesis, finding that while single mutations of Gly154 had no significant impact on MMP-3cd binding, substitutions at this position had a powerful synergistic effect when combined with the L34G mutation (**Fig. 22C-E**). To elucidate the structural basis for this synergistic effect, we co-crystallized ultra-binder TIMP-1 variants with MMP-3cd, and solved the crystal structures (**Fig. 22F**). We found that key mutation L34G brings the TIMP-1 AB-loop closer to MMP-3cd,

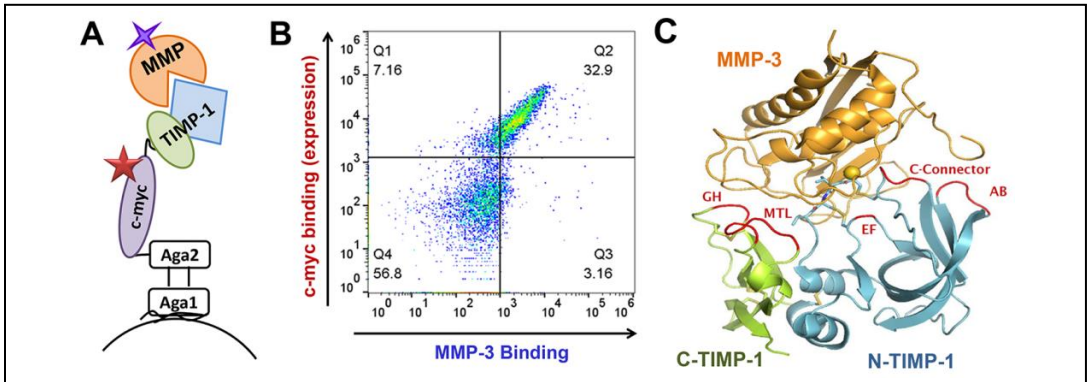

Figure 21. Yeast display of full-length TIMP-1 diversity library. (A) TIMP-1 is C-terminally fused to c-myc epitope and yeast surface protein Aga2p. TIMP-1 expression is detected with anti-c-myc and FITC-secondary antibody; MMP binding is detected with biotinylated MMP and APC-streptavidin. **(B)** Flow cytometry scatter plot shows yeast surface expression of TIMP-1 fusion construct (*y-axis*) and labeling by MMP-3 (*x-axis*). **(C)** Library diversity is focused in 17 residues of TIMP-1 (loops in red), located in both the N-terminal (*blue*) and C-terminal (*green*) domains, that interact with bound MMP-3cd (*orange*). Raeeszadeh-Sarmazdeh *et al. 2019*

cinching a reciprocal "tyrosine clasp" formed by Tyr35 of TIMP-1 and Tyr153 of MMP-3cd (**Fig. 22F**). Key mutation G154A promotes formation of an α-helical turn by TIMP-1 residues 154-157 at the interface between N- and C-terminal domains, creating a new H-bond between

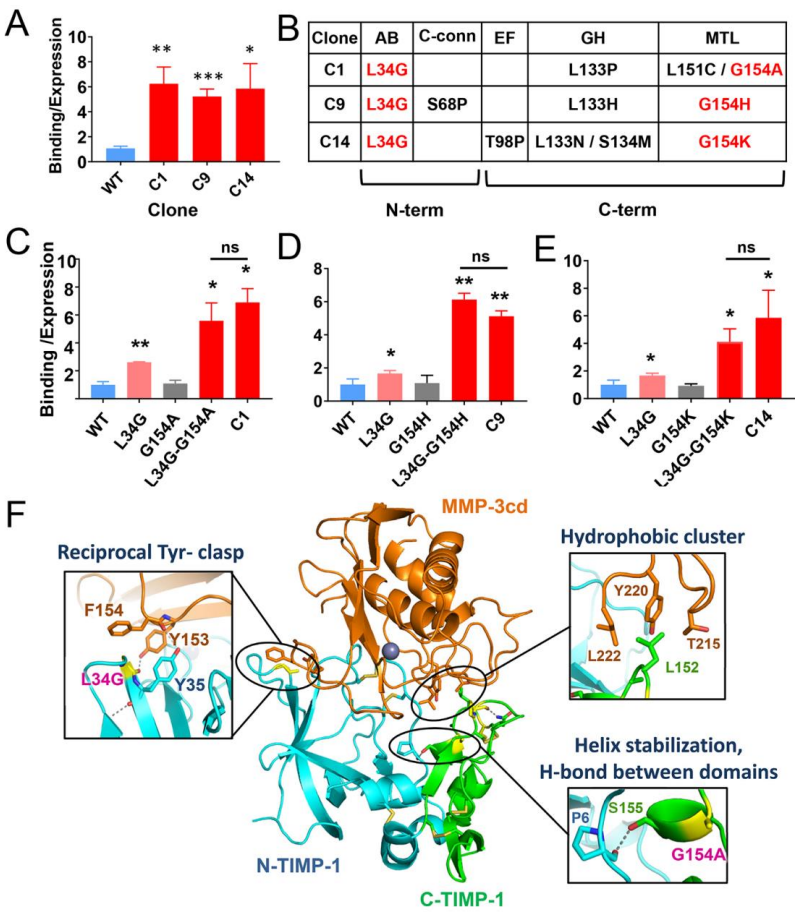

Figure 22. Distant mutations of TIMP-1 N- and C-terminal domains synergize to enhance MMP-3 binding. (A) Screening of our YSD library of TIMP-1 variants using FACS identified clones with enhanced MMP-3cd binding compared to WT-TIMP-1. **(B)** Sequencing showed that improved binders possessed 4-5 mutations spread across N- and C-terminal domains. **(C-E)** Analysis of single and double mutants showed that while L34G has a modest effect and mutations of Gly154 have no detectable effect in isolation, combining these mutations confers a synergistic enhancement of MMP-3cd binding. **(F)** Crystal structure of TIMP-1-C1 ultra-binder with MMP-3cd reveals optimized inter-domain and intermolecular interactions. L34G leads to tight cinching of a reciprocal "tyrosine clasp" (*left inset*) formed by Tyr35 of TIMP-1 and Tyr153 of MMP-3cd. G154A causes adoption of an α-helical turn by TIMP-1 residues at the interface between domains and formation of a new inter-domain H-bond (*lower right inset)*. Stabilization of TIMP-1 inter-domain interactions further leads to stabilization of hydrophobic interactions between the TIMP-1 C-terminal domain and MMP-3cd (*upper right inset*). Adapted from *Raeeszadeh-Sarmazdeh et al. 2019.*

the TIMP-1 domains (**Fig. 22F**). Stabilization of TIMP-1 inter-domain interactions promotes structural and functional integration of the two TIMP domains and leads to stabilization of hydrophobic interactions between the TIMP-1 C-terminal domain and MMP-3cd, explaining synergy between the distant mutations. Our data reveal that the C-terminal domain cooperates with the N-terminal domain to shape TIMP-1 affinity toward MMP catalytic domains, showing that holistic engineering of the full-length protein can help us to develop stronger inhibitors.

Second generation MMP-3 inhibitors based on human TIMP-1. Our first-generation MMP-3 inhibitors very potently inhibited MMP-3, however they proved to be not yet highly selective, as assessed by comparing affinities for MMP-3 and -10, the two most closely related MMP catalytic domains by sequence homology (85% identity) and structural similarity. Although we found that the MMP-3cd ultra-binder variants, which were selected exclusively for enhanced binding to MMP-3cd, were also improved binders of MMP-10cd with little discrimination between the two enzymes, we subsequently adapted our screening protocols to achieve impressively selective binders. Using a novel counter-selection strategy in which we screened our library against biotinylated MMP-3 in the presence of incremental concentrations of unlabeled MMP-10 as a competing binder in sequential rounds of FACS (**Fig. 23A**), we isolated TIMP-1 variants showing up to 26-fold improvement in selectivity for MMP-3 versus MMP-10, relative to WT TIMP-1 in the YSD context (**Fig. 23B,**C), and >13-fold preference for MMP-3 corroborated by MMP inhibition kinetics studies of the soluble TIMP variants (**Fig. 24**). Our kinetics studies also demonstrated reduced off-target activity for inhibition of MMP-9, an alternative natural target for WT TIMP-1 (**Fig. 24**).

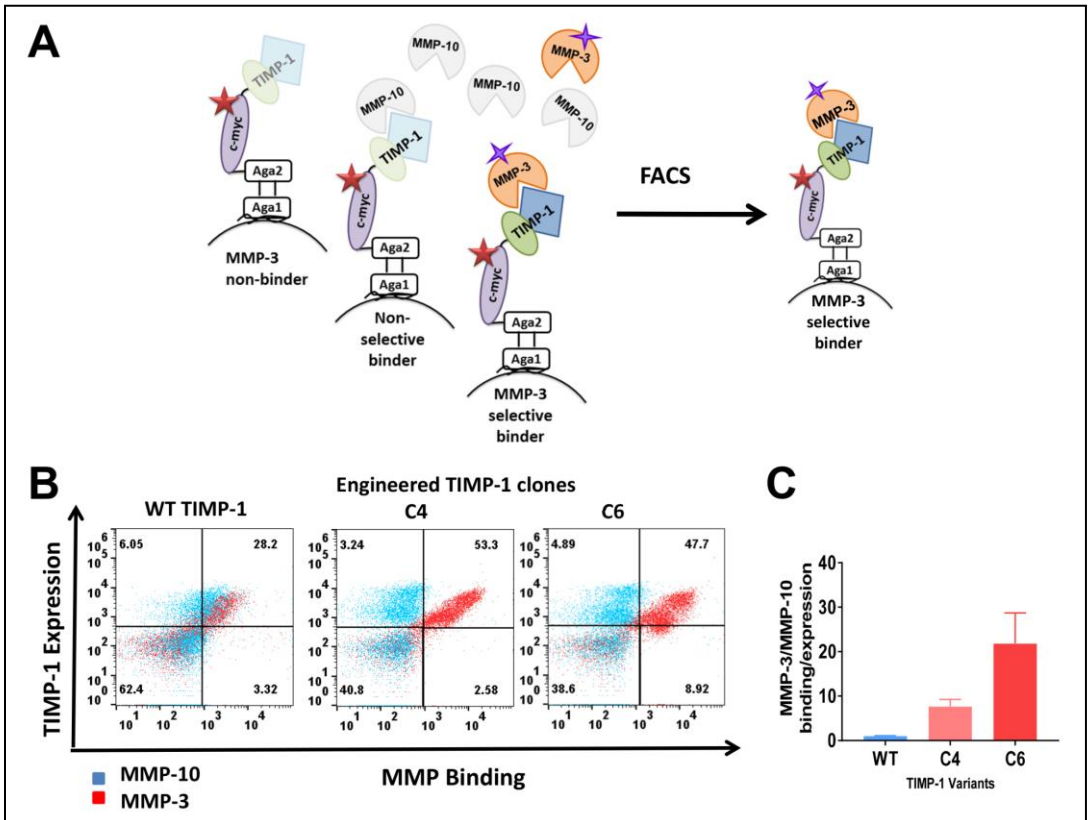

Figure 23. TIMP-1 YSD library screening yields variants selective for MMP-3 vs. MMP-10. (A) Yeast-displayed TIMP-1 library was enriched for MMP-3-selective binders by staining with biotinylated MMP-3 in the presence of increasing concentrations of unlabeled MMP-10 as a competing binder in sequential rounds of FACS. **(B)** Flow cytometry scatter plots for WT TIMP-1 (far left) show little discrimination in binding to MMP-3 (red) vs. MMP-10 (blue). Five rounds of library screening for MMP-3cd affinity in the presence of MMP-10cd competitor identified variants with highly improved selectivity, as shown by scatter plots for selective clones C4 and C6 (center and right). **(C)** Selectivity gains are quantified in bar graph.

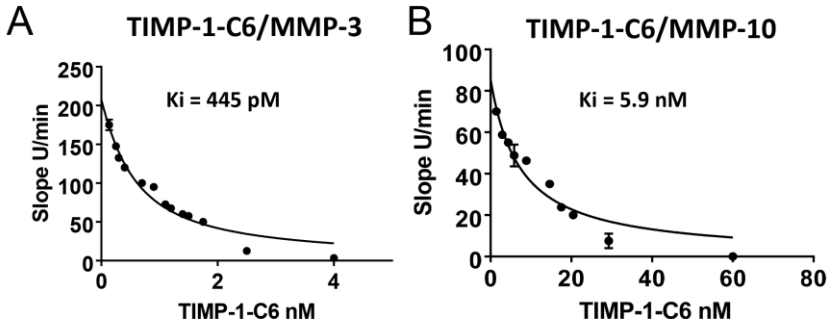

C

Ki, pM

	MMP-3	MMP-9	MMP-10
WT-TIMP1	96.4 ± 8.9	1640 ± 261	153 ± 11
TIMP-1-C6	444.7± 120.6	>> 10 nM	5947± 147.7
TIMP-1-C4	254.9 ± 18.05	>> 10 nM	4827 ± 31.5

Figure 24. MMP inhibition by soluble recombinant MMP-3-selective variants. (A) TIMP-1-C6 variant was evaluated for MMP-3 inhibition using a fluorometric substrate in the presence of increasing concentrations of the inhibitor. Data were fitted to Morrison's tight binding equation to determine an equilibrium inhibition constant (Ki) of 445 pM. **(B)** TIMP-1-C6 was found to inhibit MMP-10 with a Ki of 5.9 nM, showing >13-fold selectivity for MMP-3. **(C)** Inhibition constants (Ki) are summarized for selective variants compared to WT TIMP-1.

To elucidate the basis for specificity of selective TIMP-1 variants, we have examined sequences of variants to emerge from the selective screening protocol. We identified, in addition to the common L34G mutation found in our first-generation MMP-3 ultra-binders, the repeated presence of mutations of Met-66 (**Fig. 25A**). We have also co-crystallized TIMP-1-C6 with its target MMP-3, and solved the crystal structure at 2.3 Å resolution. This variant did not co-crystallize with the counter-target MMP-10, but we have used *in silico* mutagenesis and docking methods to model the complex, and have compared these structures to previously solved WT TIMP-1 complex structures to gain insight into selectivity. A major contributor to enhanced selectivity of TIMP-1-C6 appears to be the M66S mutation; this residue does not make critical

A

Clone	AB	C-conn	EF	GH	MTL
C4	L34G	M66D	T98G		Q153N
C5		M66G/E67N	T98D		S155L
C6	L34G	M66S/E67Y		L133N	
C9		M66G/E67H			
C10	L34G				S155L
C11	L34G	M66G/E67N			L151Q
C13	L34G	M66R			L152P/Q153C

B

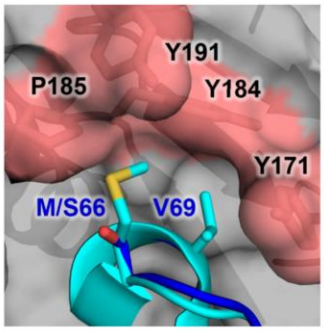

Figure 25. Loss of Met66 interactions with MMP-10 mediate improved selectivity for MMP-3. (A) Sequencing showed that selective binders possessed 2-4 mutations, with the most frequent being the common L34G mutation and various substitutions for Met66. **(B)** TIMP-1/MMP-10 crystal structure shows tight packing of TIMP-1 Met66 (*cyan*) with hydrophobic MMP-10 exosite residues (*salmon*), interactions that are lost in the model with MMP-3-selective TIMP-1-C6, featuring the M66S mutation (*blue*).

contacts in the MMP-3cd complex, but its mutation disrupts crucial hydrophobic interactions with an MMP-10 exosite (**Fig. 25B**).

Major Task 3. Determine if levels of MMP-3 and MMP-3 proteolytic products are elevated in the lungs and blood of patients with pulmonary fibrosis and in military personnel previously deployed to Southwest Asia and can be used as a biomarker for disease progression. (This section is from Dr. Downey at National Jewish Health and Dr. Radisky at Mayo Clinic)

Subtask 1. Local IRB Approval

We obtained local (National Jewish Health) RRB approval on 11/29/2016 (NJH protocol # HS3012) to use archived blood and bronchoalveolar lavage samples.

We then obtained approval from the University of Colorado IRB (CoMIRB) on 1/19/2017 (CoMIRB protocol #16-2661) to use existing formalin-fixed lung biopsy samples (obtained by video-assisted thoracoscopic (VATS) biopsy) stored at the University of Colorado Hospital.

Subtask 2. USAMRMC IRB/HRPO Approval for human subjects.

We obtained USAMRMC IRB/HRPO approval on 03/2/2017 to conduct analysis on blood serum samples from idiopathic pulmonary fibrosis patients at the National Jewish Health and analysis of 10 archived lung biopsies samples from symptomatic military personnel previously deployed to Southwest Asia collected under standard care procedures at the University of Colorado Hospital.

Subtask 3. Determine if MMP-3 and osteopontin peptide levels are elevated in serum from patients with deployment lung disease.

We analyzed MMP-3 levels in blood samples from 10 normal human donors and 10 previously deployed military personnel (deployers) using an ELISA. The levels in both normal human donors and deployers were low (1.1 - 4.2 ng/ml) and there were no significant differences between the groups.

Subtask 4. Analyze the chemical and mineralogical composition and anatomic location of PM from VATS lung biopsies and alveolar macrophages obtained by BAL from deployed military personnel.

Over the last year, Dr. Geoff Plumlee and Ms. Heather Lowers at the United States Geological Survey (USGS) have continued to refine their methods to measure levels of particulate matter and chemical content of biological fluids and tissues including bronchoalveolar lavage fluid and whole lung tissue. This part of the project has encountered several hurdles and setbacks. Due to the COVID-19 pandemic, the USGS has either been closed or running on skeleton staff since March 2020. Despite these circumstances, they have made significant progress on developing methods to digest isolated lung lavage cells and lung tissue using highly purified hydrogen peroxide (H_2O_2). We found that most commercial preparations of H_2O_2 contained high levels of tin and other trace metals that were added to stabilize the H_2O_2 that is otherwise highly reactive and unstable in solution.

We reasoned that we would refine the methods to digest and analyze whole lung tissue using the lungs of mice that had been treated with PM from Afghanistan, Iraq, and California before using the valuable and limited surgical lung biopsies from previously deployed military personnel. Accordingly, the USGS completed a series of studies to measure the levels of PM and the elemental composition of the lungs of mice that had PM from Afghanistan and Iraq and

California (China Lake) instilled by oropharyngeal instillation. For this analysis, they used inductively coupled plasma mass spectrometry (ICP-MS). These studies are summarized below in **Figure 26** and **Table 1**. Notably, the concentrations of some of the elements are very low in concentration and below the levels in the blanks (**Figure 26**). These studies indicate that silicate-containing PM can be detected in BAL fluid and lung tissue although the levels present for some metals are close to the limits of detection. We are awaiting the completion of methods development before using the human deployer VATS biopsy samples. This part of the analysis will be supported by our other DoD grant: 'Mechanisms and Treatment of Deployment-Related Lung Injury: Repair of the Injured Epithelium' (W81XWH-16-2-0018; PR150109).

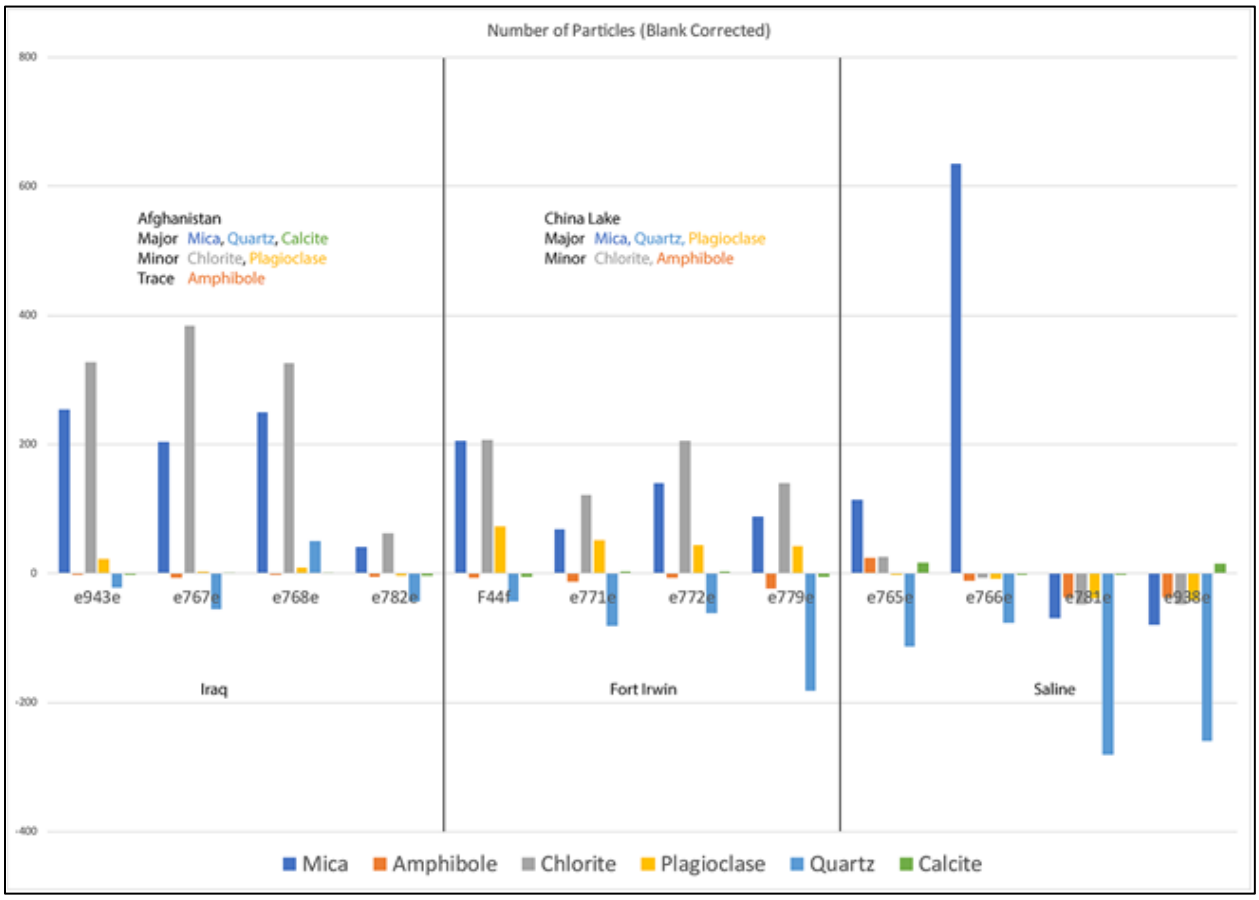

Figure 26. ICP-MS results from lungs of mice instilled with PM from Iraq, Afghanistan, or China Lake.

Slice_thickness_(um)	0	40	40	40	40	40	40	40	40	40	40	40	40
Slice_area_(cm2)	0.00	0.00	0.00	0.00	0.00	0.00	0.00	0.00	0.00	0.00	0.00	0.00	0.00
Slice_volume_(cm3)		1.0000	1.0000	1.0000	1.0000	1.0000	1.0000	1.0000	1.0000	1.0000	1.0000	1.0000	1.0000
Filter_(g)	0.0373	0.0381	0.0392	0.0414	0.0420	0.0422	0.0377	0.0382	0.0389	0.0401	0.0408	0.0424	0.0408
Tissue+Filter_(g)	0.0373	0.0456	0.0464	0.0555	0.0496	0.0502	0.0542	0.0459	0.0475	0.0471	0.0553	0.0503	0.0506
Filter_+_Tissue_(g)_after_xylene_and_dry_overnight	0.0367	0.0376	0.0388	0.0409	0.0415	0.0419	0.0372	0.0380	0.0386	0.0397	0.0402	0.0422	0.0404
Weight_of_tissue_(g)	-0.0006	0.0001	0.0002	0.0001	0.0001	0.0003	0.0001	0.0004	0.0003	0.0002	0.0000	0.0004	0.0002
Suspension_volume_(mL)	25	25	25	25	25	25	25	25	25	25	25	25	25
Aliquote_volume_(uL)	25000	25000	25000	25000	25000	25000	25000	25000	25000	25000	25000	25000	25000
Fraction_of_suspension_	1.0000	1.0000	1.0000	1.0000	1.0000	1.0000	1.0000	1.0000	1.0000	1.0000	1.0000	1.0000	1.0000
Active_area_filter_(mm2)	181	181	181	181	181	181	181	181	181	181	181	181	181
field area (um)	48	48	48	48	48	48	48	48	48	48	48	48	48
field height (um)	42	42	42	42	42	42	42	42	42	42	42	42	42
field area (um)	2025	2025	2025	2025	2025	2025	2025	2025	2025	2025	2025	2025	2025
# of fields completed	56	18	20	7	12	26	22	26	44	34	19	55	54
Fraction of filter examined	0.0006	0.0002	0.0002	0.0001	0.0001	0.0003	0.0002	0.0003	0.0005	0.0004	0.0002	0.0006	0.0006
Total # particles	1089	973	913	976	314	986	745	919	827	913	957	352	470
Total #geologic material	692.0000	845.0000	780.0000	743.0000	197.0000	745.0000	422.0000	660.0000	579.0000	605.0000	831.0000	137.0000	156.0000
Total particles/cm3	#DIV/0!	4.8E+06	4.1E+06	1.2E+07	2.3E+06	3.4E+06	3.0E+06	3.2E+06	1.7E+06	2.4E+06	4.5E+06	5.7E+05	7.8E+05
Ag_phase	1	0	0	0	0	0	0	0	0	0	0	0	0
Al_oxide	41	1	1	6	0	18	2	3	6	15	2	5	9
Al_oxide_mix	15	2	2	0	0	3	0	0	1	17	5	0	2
Al_P_phase	0	1	0	0	1	0	1	0	0	0	3	0	0
Al_S_phase	0	0	0	1	0	1	0	0	0	0	0	0	0
Aluminosilicate_Al_gt_Si	15	3	3	7	2	10	0	1	3	29	231	3	3
Aluminosilicate_Al_lt_Si	68	137	146	186	26	168	67	97	84	116	430	23	13
Au_phase	2	0	0	0	0	0	0	0	2	2	1	0	0
Ba_phase	1	1	0	0	0	0	0	1	0	0	0	1	0
C_Cl	35	11	6	13	12	45	33	45	45	34	8	24	24
Ca_Al_oxide	0	0	1	0	0	0	0	0	0	3	0	0	0
Ca_Al_silicate	11	5	4	3	2	1	2	5	2	61	13	0	0
Ca_Mg_Al_Si	1	0	0	1	0	1	0	1	0	22	0	0	0
Ca_Mg_Fe_Al_silicate	11	2	0	0	0	2	1	0	1	2	0	0	0
Ca_Mg_Fe_silicate	9	2	0	0	1	3	1	3	2	4	2	0	0
Ca_Mg_phase	0	0	2	0	1	1	2	2	0	1	0	0	0
Ca_Mg_silicate	9	0	0	0	0	3	0	2	2	2	0	1	0
Ca_Mg_Ti_Al_Si	0	0	0	0	0	0	0	0	0	3	0	0	0
Ca_P_phase	0	0	0	1	1	2	8	0	1	0	0	0	0
Ca_P_phase_mix	1	0	1	0	1	1	2	1	0	1	0	0	0
Ca_phase	13	3	5	2	0	1	7	8	5	24	2	11	27
Ca_phase_mix	5	2	1	0	0	0	0	1	0	8	0	0	2
Ca_silicate	5	0	0	0	0	0	0	2	5	8	1	2	0
Ca_Ti_oxide	1	0	0	0	0	0	0	0	0	0	0	0	0
CaCl2	18	0	1	2	10	24	32	50	11	24	4	24	3
Carbonaceous	138	28	45	165	10	83	197	66	97	96	69	91	153
Carbonaceous_NoO	11	2	7	4	6	1	6	2	8	7	0	11	8
Cr_phase	4	2	0	0	0	2	6	3	2	2	3	3	2
Cu_phase	0	0	1	0	2	0	0	0	0	1	0	0	0
Fe_aluminosilicate	4	9	16	5	4	2	3	5	12	6	0	0	1
Fe_Cr	16	1	0	0	0	0	0	2	4	2	0	2	9
Fe_Ni	9	0	1	0	1	2	0	4	3	5	4	3	18
Fe_Ni_Cr	2	2	0	0	0	0	0	0	2	0	0	0	6
Fe_oxide	53	23	15	12	2	32	15	30	32	44	7	22	51
Fe_oxide_mix	32	50	42	29	18	24	20	38	23	41	14	16	5
Fe_silicate	6	3	2	1	1	3	1	4	2	1	1	1	0
Fe_Ti_oxide	0	0	0	0	0	1	0	0	0	3	0	0	0
Fe_Ti_oxide_mix	0	1	1	0	0	0	0	0	1	0	0	0	0
Feldspar_	1	0	0	0	0	0	0	0	0	0	0	0	0
Feldspar_K	15	25	13	11	3	73	50	45	50	13	6	8	5
Feldspar_Na	12	10	6	4	5	17	16	19	17	14	1	5	3
Feldspar_NaK	2	4	3	1	0	3	2	3	6	1	1	2	1
Feldspar_Plag	26	2	1	0	0	5	6	3	13	5	3	1	3
K_aluminosilicate	27	149	94	70	37	78	45	92	87	36	11	13	11
Mafic	9	7	7	3	3	3	1	6	2	18	0	0	0
Mg_aluminosilicate	5	85	128	128	19	105	65	76	42	13	2	3	2
Mg_Fe_aluminosilicate	46	238	251	190	49	119	70	144	127	39	9	10	6
Mg_Fe_phase	3	1	0	0	0	0	5	4	3	7	6	2	7
Mg_Fe_Silicate	8	1	0	2	0	3	0	3	5	1	4	0	1
Mg_phase	0	1	0	1	0	0	2	3	1	1	1	0	0
Mg_silicate	1	15	11	9	3	7	8	7	4	5	0	2	4
Mn_phase	0	1	0	0	0	0	0	0	0	0	0	0	0
Na_K_Ca_S_Cl	5	1	5	0	2	0	6	2	5	2	3	0	2
Na_P_phase	0	0	0	0	1	0	0	0	0	0	0	0	0
NaCl	1	0	1	0	0	0	0	6	0	0	0	0	2
Ni_phase	7	0	1	0	0	1	0	1	1	1	0	0	6
P_phase	1	0	0	0	0	0	0	0	0	0	0	0	0
REE	0	0	0	0	0	0	0	0	1	0	0	0	0
S_phase	0	0	1	0	0	0	0	0	0	0	0	0	0
Silica	226	59	45	70	24	79	35	60	58	69	30	31	54
Silica_mix	101	24	16	20	3	30	12	30	17	17	5	9	2
Sn_phase	1	0	0	0	51	4	1	1	5	2	2	14	12
Ti_Fe_oxide	0	4	0	1	0	0	1	1	1	3	8	0	2
Ti_Fe_oxide_mix	1	6	0	1	0	0	0	0	1	2	0	0	0
Ti_oxide	29	25	8	10	6	13	6	13	12	42	28	7	9
Ti_oxide_mix	23	22	18	13	6	10	6	19	12	33	36	2	2
Titanite	0	2	0	2	0	2	2	2	1	3	0	0	0
Zr_phase	2	0	1	2	1	0	0	3	0	2	1	0	0

Table 1. ICP-MS results from lungs of mice instilled with PM from Iraq, Afghanistan, or China Lake and the digested with H_2O_2 prior to analysis.

We have completed experiments examining the effects of *in vitro* exposure to particulate matter on fibrogenic gene expression in primary human alveolar macrophages isolated from the lungs or organ donors not used for transplant. We used RNASeq to quantify the fibrogenic gene expression in these alveolar macrophages exposed to particulate matter from Afghanistan and Iraq. These experiments were also supported in part by our other DoD grant: 'Mechanisms and Treatment of Deployment-Related Lung Injury: Repair of the Injured Epithelium' (W81XWH-16-2-0018; PR150109).

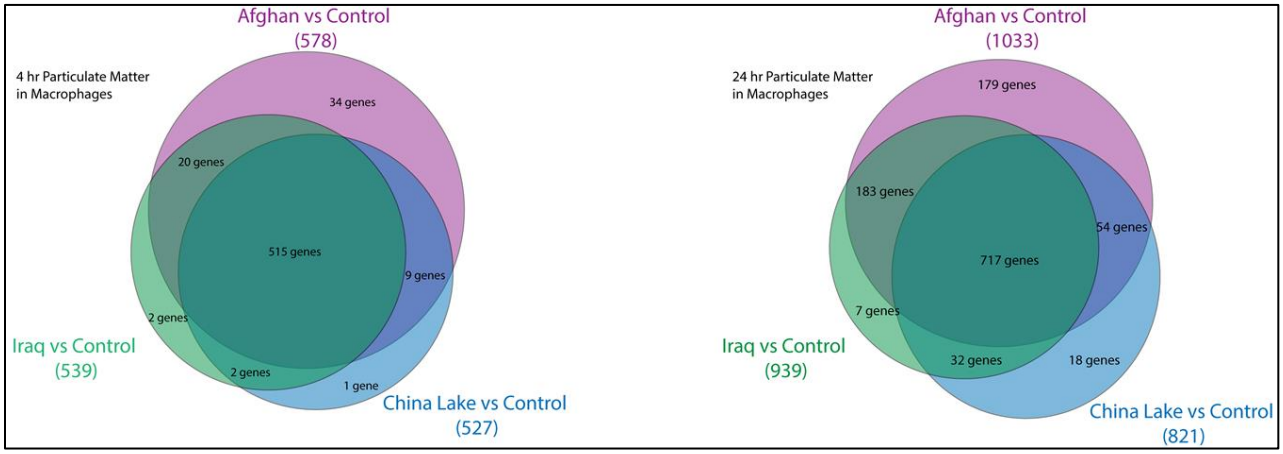

Figure 27. Analysis of differential gene expression in human primary alveolar macrophages exposed to PM (10 μg/cm^2) from Iraq, Afghanistan and California *in vitro*.

As illustrated in **Fig. 27**, exposure of human alveolar macrophages to PM from Iraq, Afghanistan, and China Lake induced differential expression of 500-1000 genes at 4 and 24 hr compared to control (saline). Of these genes, 515 were in common at 4 hr and 717 at 24 hr indicating common responses the PM independent of the geographic source of PM. By contrast, at 24 hr there were 179 unique genes expressed in response to PM from Afghanistan and 9 unique genes expressed in response to PM from Iraq.

Ingenuity Pathway Analysis revealed the macrophages responded to PM exposure by expression of a variety of acute inflammatory pathways including rheumatoid arthritis pathway (this is a pathway highly enriched in inflammatory signaling through IL-1β and TNFα) , TNFR1 and IL-6 signaling, acute phase response signaling (**Fig. 28**).

Figure 28. Pathway analysis of RNAseq using Ingenuity Pathway Analysis tool of differential gene expression in human primary alveolar macrophages exposed to PM (10 µg/cm^2) from Afghanistan *in vitro*.

Additional bioinformatics analysis revealed a strong signal in the NFκB pathway (**Fig. 29**) that is known to control signaling pathways involved on acute inflammatory responses and is a major target of glucocorticoids. This has important implications for potential therapeutic interventions for example with inhaled glucocorticoids that are currently used for a variety of human respiratory diseases such as asthma. We validated several of the genes most highly upregulated using qPCR to ensure that the signal in RNAseq was not an artifact.

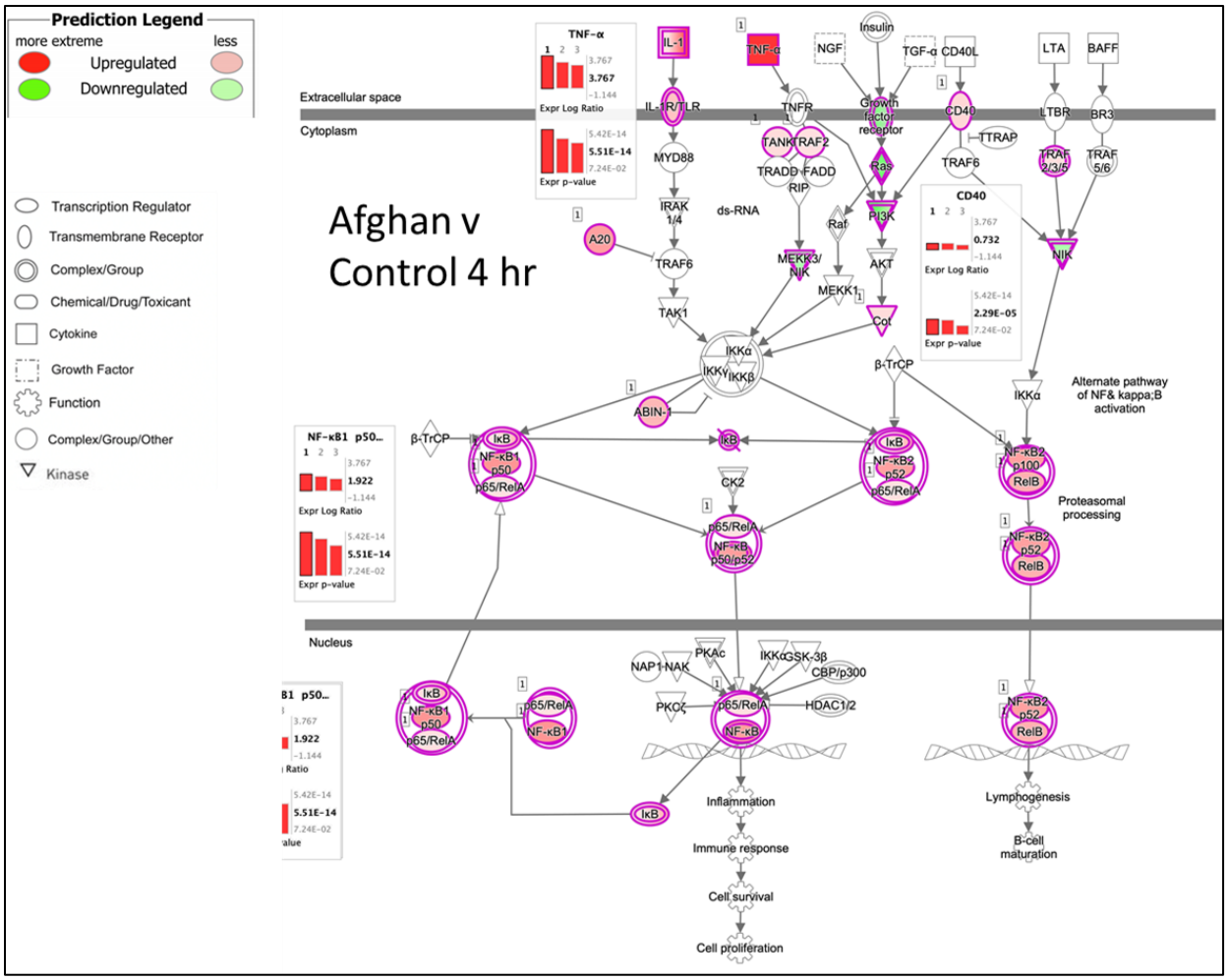

Figure 29. Pathway analysis of RNAseq using Ingenuity Pathway Analysis tool of differential gene expression in human primary alveolar macrophages exposed to PM (10 µg/cm^2) from Afghanistan *in vitro* reveals activation of the NFκB pathway that is a key controller of inflammation.

Subtask 5. Prepare and submit manuscripts for publication.

We have published two manuscripts to date:

1. Raeeszadeh-Sarmazdeh M, Greene KA, Sankaran B, **Downey GP**, **Radisky D**, Radisky Y. Directed evolution of metalloproteinase inhibitor TIMP-1 reveals cooperation between domains in matrix metalloproteinase recognition. J Biol Chem 2019;294(24):9476-9488. doi: 10.1074/jbc.RA119.008321

2. Garshick E, Abraham J, Baird C, Ciminera P, **Downey GP**, Falvo MJ, Hart JE, Jackson DA, Jerrett M, Kuschner W, Helmer DA, Jones KD, Krefft SD, Mallon T, Miller RF, Morris MJ, Proctor SP, Redlich CA, **Rose CS**, Rull, RP, Saers J, Schneiderman AI, Smith NL, Smith NL, Yiallouros P, Blanc PD. Respiratory Health after Military Service in Southwest Asia and Afghanistan. An Official American Thoracic Society Workshop Report. Ann Am Thorac Soc. 2019 Aug;16(8):e1-e16. doi: 10.1513/AnnalsATS.201904-344WS.

What opportunities for training and professional development has the project provided?

Dr. Maryam Raeeszadeh-Sarmazdeh, a postdoc in the E. Radisky laboratory working on the TIMP-1 engineering project, attended and her presented research at three conferences and has published one manuscript. Daniel Foster, a senior Research Associate in Dr. Downey's laboratory presented the bioinformatics analysis at the University of Colorado city-wide research rounds. Based on his interest in this area, Mr. Foster recently began his Ph.D. program in Toxicology at the University of Colorado Anschutz Campus.

How were the results disseminated to communities of interest?

Poster presentations and podium talks were presented at the annual MHSRS meetings in 2018 and 2019 in Orlando and Drs. Downey and Rose participated in a workshop at the annual meeting of the American Thoracic Society in 2018 on Deployment Lung Disease that lead to a publication in the Annals of the American Thoracic Society.

What do you plan to do during the next reporting period to accomplish the goals?

Nothing to report

4. **IMPACT:** Describe distinctive contributions, major accomplishments, innovations, successes, or any change in practice or behavior that has come about as a result of the project relative to:

What was the impact on the development of the principal discipline(s) of the project?

We have demonstrated that exposure of mice to silicate-containing PM induces pulmonary fibrosis with initial inflammation in the terminal bronchioles and alveolar ducts followed by collagen deposition. We have demonstrated that human alveolar macrophages respond to inhaled particulate matter by producing an array of inflammatory and fibrogenic mediators that likely contribute to the respiratory symptoms and clinical illness frequently observed in military personnel previously deployed to Southwest Asia and Afghanistan.

What was the impact on other disciplines?

We have demonstrated the feasibility of engineering highly selective TIMP-based MMP inhibitors by yeast surface display. We expect this result to impact the field of protein engineering. Our efforts to uncover the sequence and structural determinants responsible for improvements in TIMP-1 selectivity will also impact the understanding of protein-protein interactions and binding specificity.

What was the impact on technology transfer?

Nothing to report

What was the impact on society beyond science and technology?

Nothing to report

5. **CHANGES/PROBLEMS:** The Project Director/Principal Investigator (PD/PI) is reminded that the recipient organization is required to obtain prior written approval from the awarding agency Grants Officer whenever there are significant changes in the project or its direction. If not previously reported in writing, provide the following additional information or state, "Nothing to Report," if applicable:

Changes in approach and reasons for change

Our method to expose mice to aerosolized silicate-containing PM or to purified silica resulted in low levels of inflammation and minimal fibrosis whereas bypass of the mouse nasopharynx using the technique of oropharyngeal aspiration to deliver materials directly to the lung results in in significant inflammation and fibrosis. Thus we have used oropharyngeal aspiration as our primary method of exposure. This has the advantage that the exposures can be done at our local institution instead of having to ship mice to and from Dayton, Ohio. We have also encountered difficulty in measuring the PM and metal content of lung tissue. In collaboration the US Geological Survey, we have developed novel ways to digest lung tissue using H_2O_2 that enables measurement of very low levels of particulates and metals in the lung.

Actual or anticipated problems or delays and actions or plans to resolve them

Transfer of funds from the DoD to NAMRU-Dayton was delayed both initially in 2016 and again in 2019. This led to short delays in obtaining local IACUC and then ACURO approval for the animal experiments involving inhalational exposure of mice to silicate-containing particulate matter (PM) and in conducting the experiments. We have now received funds and experiments have been completed.

Changes that had a significant impact on expenditures

The COVID-19 pandemic slowed down progress in the last 10 months. This was particularly severe for the studies with the US Geological Survey because their laboratories were either closed or on skeleton staffing for at least 6 months.

Significant changes in use or care of human subjects, vertebrate animals, biohazards, and/or select agents

Significant changes in use or care of human subjects

No significant changes

Significant changes in use or care of vertebrate animals.

No significant changes

Significant changes in use of biohazards and/or select agents

No significant changes

6. PRODUCTS: List any products resulting from the project during the reporting period. If there is nothing to report under a particular item, state "Nothing to Report."

- **Publications, conference papers, and presentations**
  Report only the major publication(s) resulting from the work under this award.

  Journal publications.

1. Raeeszadeh-Sarmazdeh M, Greene KA, Sankaran B, Downey GP, Radisky D, Radisky E.S. Directed evolution of metalloproteinase inhibitor TIMP-1 reveals cooperation between domains in matrix metalloproteinase recognition. J Biol Chem 2019;294(24):9476-9488. doi: 10.1074/jbc.RA119.008321.

2. Garshick E, Abraham J, Baird C, Ciminera P, **Downey GP**, Falvo MJ, Hart JE, Jackson DA, Jerrett M, Kuschner W, Helmer DA, Jones KD, Krefft SD, Mallon T, Miller RF, Morris MJ, Proctor SP, Redlich CA, **Rose CS**, Rull, RP, Saers J, Schneiderman AI, Smith NL, Smith NL, Yiallouros P, Blanc PD. Respiratory Health after Military Service in Southwest Asia and Afghanistan. An Official American Thoracic Society Workshop Report. Ann Am Thorac Soc. 2019 Aug;16(8):e1-e16. doi: 10.1513/AnnalsATS.201904-344WS.

Books or other non-periodical, one-time publications.

Nothing to Report

Other publications, conference papers, and presentations.

1. Maryam Raeeszadeh-Sarmazdeh, Banumathi Sankaran, Derek C. Radisky, Evette S. Radisky. Structural Elucidation of Engineered Tissue Inhibitor of Metalloproteinases-1 (TIMP-1) Variants with Improved Binding Affinity toward Matrix Metalloproteinase-3 (MMP-3). ASBMB Annual Meeting, Orlando, FL, April 2019 (poster).
2. Maryam Raeeszadeh-Sarmazdeh, Matt Coban, Banumathi Sankaran, Radisky E.S. Structural elucidation of engineered tissue inhibitor of metalloproteinase -1 (TIMP-1) variants with improved binding affinity toward matrix metalloproteinase-3 (MMP-3). ACS Annual Meeting, Orlando, FL, April 2019 (oral presentation).
3. Maryam Raeeszadeh-Sarmazdeh, Matt Coban, Banumathi Sankaran, Radisky E.S. Directed evolution of the tissue inhibitor of metalloproteinases-1 (TIMP-1) scaffold for developing selective therapeutic agents. ACS Annual Meeting, Orlando, FL, April 2019 (poster and short talk).
4. Maryam Raeeszadeh-Sarmazdeh, Matt Coban, Banumathi Sankaran, Radisky E.S. Directed evolution of the metalloproteinase inhibitor TIMP-1 reveals cooperation between domains in matrix metalloproteinase recognition. Gordon Research Conference – Metalloproteases, Il Ciocco, Barga, Tuscany, Italy, May 2019 (poster).

- **Website(s) or other Internet site(s)**

Nothing to Report

- **Technologies or techniques**

We have developed and optimized protocols for selectivity screening of yeast surface displayed TIMP-1 libraries; this methodology will be shared in published research papers.

- **Inventions, patent applications, and/or licenses**

Nothing to Report

- **Other Products**

We have developed preclinical animal models of pulmonary fibrosis induced by exposure to silicate containing particulate matter that reflect deployment related exposures to military personnel.

7. PARTICIPANTS & OTHER COLLABORATING ORGANIZATIONS

What individuals have worked on the project?

Name: Gregory Downey, MD
Project Role: Principal Investigator
Researcher Identifier (e.g. ORCID ID): 0000-0003-3253-5862
Nearest person month worked: 1 (annually)
Contribution to Project: Dr. Downey is the PI at the National Jewish Site. as planned and overseen experiments including preclinical models of exposure to silicate-containing particulate matter.

Name: Daniel Foster
Project Role: Lab Researcher
Researcher Identifier (e.g. ORCID ID): N/A
Nearest person month worked: 2 (annually year three)
Contribution to Project:

Name: Geoffrey Plumlee
Project Role: Site PI USGS
Researcher Identifier (e.g. ORCID ID): N/A
Nearest person month worked: <1 (annually)
Contribution to Project: Dr. Plumlee has been responsible for measurement of the particle size and content of silica and particulate matter from Iraq, Afghanistan and California.

Name: Heather Lowers
Project Role: Co-Investigator
Researcher Identifier (e.g. ORCID ID): N/A
Nearest person month worked: 1 month (annually)
Contribution to Project: This participant is responsible for sample handling and logistics, SEM analysis, XRD summary, particle size analysis, and report writing

Name: Bill Benzel
Project Role: Researcher
Researcher Identifier (e.g. ORCID ID): N/A
Nearest person month worked: 1 month (annually)
Contribution to Project: This participant is responsible for XRD analysis and particle size analysis

Name: Kate Campbell
Project Role: Researcher
Researcher Identifier (e.g. ORCID ID): N/A

Nearest person month worked: 1 month (annually)
Contribution to Project: This participant is responsible for sample handling and ICP-MS method development

Name: David Roth
Project Role: Researcher
Researcher Identifier (e.g. ORCID ID): N/A
Nearest person month worked: 1 month (annually)
Contribution to Project: This participant is responsible for ICP-MS method development and sample analysis

Name: Nour Hanandeh
Project Role: Contractor/Engineer
Nearest person month worked: 1 (annually)
Contribution to project: Operating wright dust feeder for generation/collection of sand/silica particles.

Name: Derek Radisky
Project Role: Partner PI
Researcher Identifier (e.g. ORCID ID):
Nearest person month worked: 2 (annually)
Contribution to Project: Dr. Downey is the partnering PI at the Mayo Clinic Jacksonville site. Dr. Radisky has been responsible for the planning and oversight of the experiments on the recombinant TIMP-1 variants.

Name: Evette S. Radisky
Project Role: Co-Investigator
Researcher Identifier (e.g. ORCID ID): N/A
Nearest person month worked: 1
Contribution to Project: Dr. E. Radisky supports the planning and execution of the recombinant TIMP-1 variants experiments.

Name: Maryam Raeeszadeh Sarmazdeh
Project Role: Postdoctoral Fellow
Researcher Identifier (e.g. ORCID ID): N/A
Nearest person month worked: 4
Contribution to Project: Performs TIMP selection, production, and characterization.

Name: Erin Miller
Project Role: Technician
Researcher Identifier (e.g. ORCID ID): N/A
Nearest person month worked: 1
Contribution to Project: Provides support for TIMP selection.

Name: Melody Stallings Mann
Project Role: Technician
Researcher Identifier (e.g. ORCID ID): N/A
Nearest person month worked: 1
Contribution to Project:

Has there been a change in the active other support of the PD/PI(s) or senior/key personnel since the last reporting period?

Nothing to report

What other organizations were involved as partners?

Organization Name: Mayo Clinic Jacksonville
Location of Organization: (if foreign location list country) Jacksonville, FL
Partner's contribution to the project (identify one or more) Partnering PI

- Dr. Radisky has been responsible for the design and generation of recombinant TIMP-1 variants.
- Dr. Radisky visited National Jewish Health on March 8, 2017 to discuss the project progress and future plans.

Organization Name: NAMRU Dayton
Location of Organization: (if foreign location list country) Dayton, Ohio
Partner's contribution to the project (identify one or more) Collaboration on inhalational toxicology

Organization Name: United States Geological Survey (USGS)
Location of Organization: (if foreign location list country) Reston, VA and Lakewood, CO
Partner's contribution to the project (identify one or more)

- The USGS has carried out mineralogical and particle size distribution analyses of the crystalline silica standard to be used in in vitro and in vivo tests by NJH
- The USGS is currently performing mineralogical and particle size distribution analyses of the Iraq dust sample to be used in in vitro and in vivo tests by NJH
- The USGS and NJH have worked together to develop a plan for chemical analyses of materials from *in vitro* dosing tests, to examine uptake of metals and other components from the dosing materials by the test cells.

8. SPECIAL REPORTING REQUIREMENTS

COLLABORATIVE AWARDS: For collaborative awards, independent reports are required from BOTH the Initiating PI and the Collaborating/Partnering PI. A duplicative report is acceptable; however, tasks shall be clearly marked with the responsible PI and research site. A report shall be submitted to **https://ers.amedd.army.mil** for each unique award.

QUAD CHARTS: If applicable, the Quad Chart (available on https://www.usamraa.army.mil) should be updated and submitted with attachments.

Not applicable

9. APPENDICES:

Attach all appendices that contain information that supplements, clarifies or supports the text. Examples include original copies of journal articles, reprints of manuscripts and abstracts, a curriculum vita, patent applications, study questionnaires, and surveys, etc.